DE LA RECHERCHE À L'INDUSTRIE

www.cea.fr

# *EXPLORING THE ENERGY LANDSCAPE*

**Mihai-Cosmin Marinica**

**CEA, DEN, Service de Recherches de Métallurgie Physique, Saclay, France**

**mihai-cosmin.marinica@cea.fr**

# Introduction

The goal is to have the values for transition rates

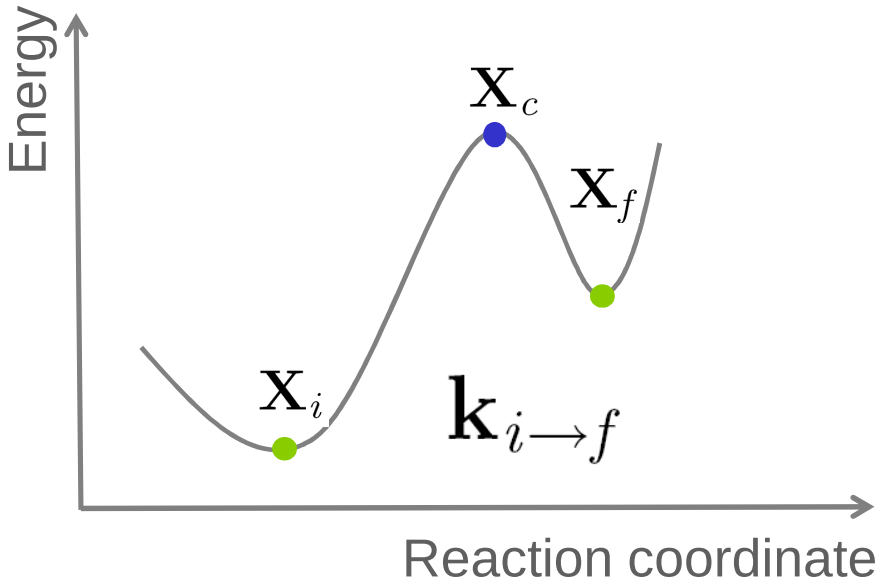


… which can be used in any large scale is time and space simulation:

1. Rate theory
2. AKMC,
3. OKMC,
4. EKMC (JERK, FPKMC)
5. …

# Introduction

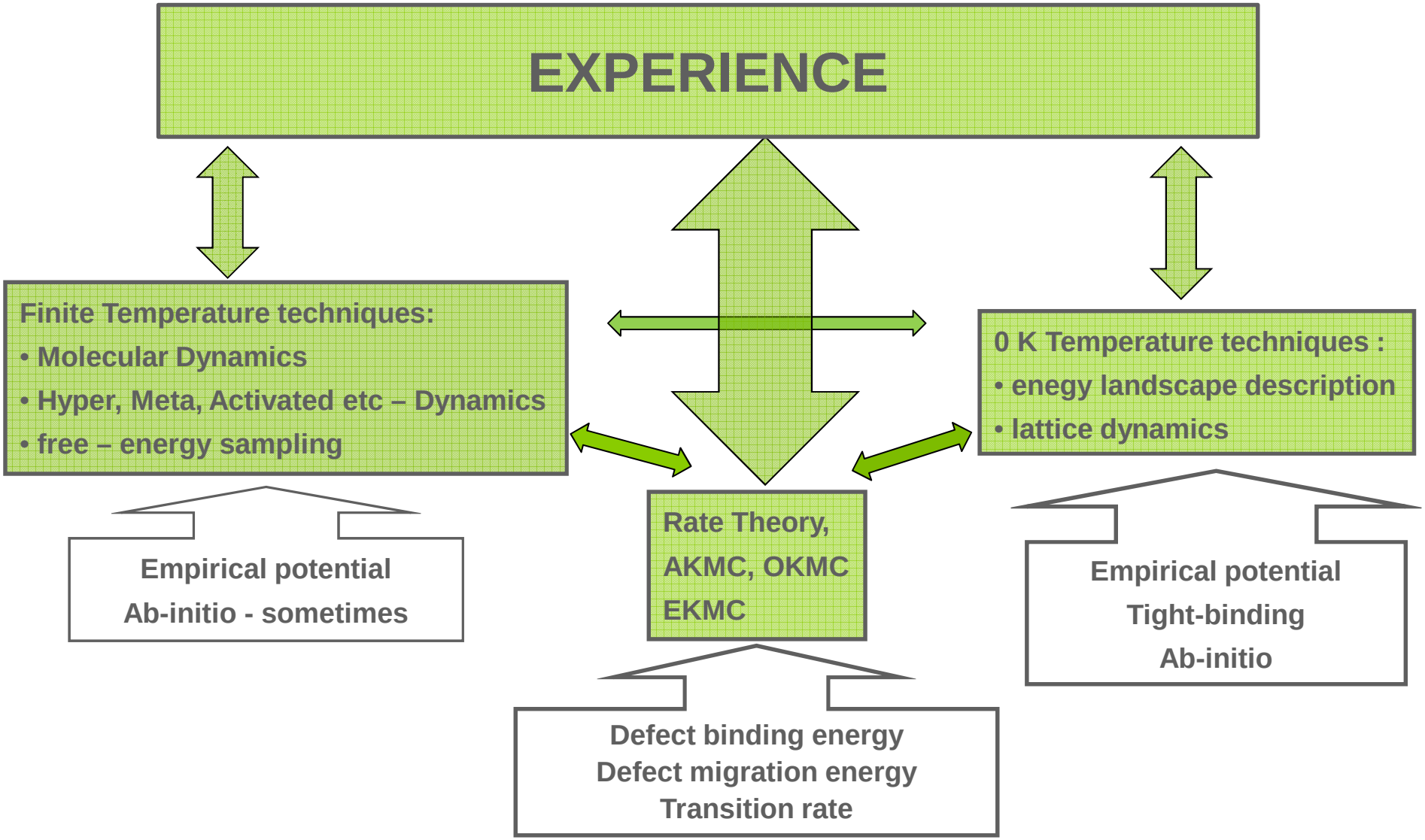

# Introduction

$$H(q,p) = \frac{1}{2} p^T M^{-1} p + V(q) \qquad M = \mathrm{Diag}(m_1, \ldots, m_N) \qquad q = (q_1, \cdots, q_N) \in \mathbb{R}^{3N}$$

$$(p_1, \ldots, p_N) \in \mathbb{R}^{3N}$$

$$\langle A \rangle = \int_{\mathcal{M}^N \times \mathbb{R}^{3N}} A(q,p)\, d\mu(q,p).$$

$$d\mu(q,p) = Z^{-1} \exp(-\beta H(q,p))\, dq\, dp,$$

$$Z = \int_{T^*\mathcal{M}} \exp(-\beta H(q,p))\; dq\, dp.$$

$$\begin{cases} \dot{q}_i(t) = \dfrac{\partial H}{\partial p_i}(q(t),p(t)) = \dfrac{p_i(t)}{m_i}, \\ \dot{p}_i(t) = -\dfrac{\partial H}{\partial q_i}(q(t),p(t)) = -\nabla_{q_i} V(q(t)). \end{cases}$$

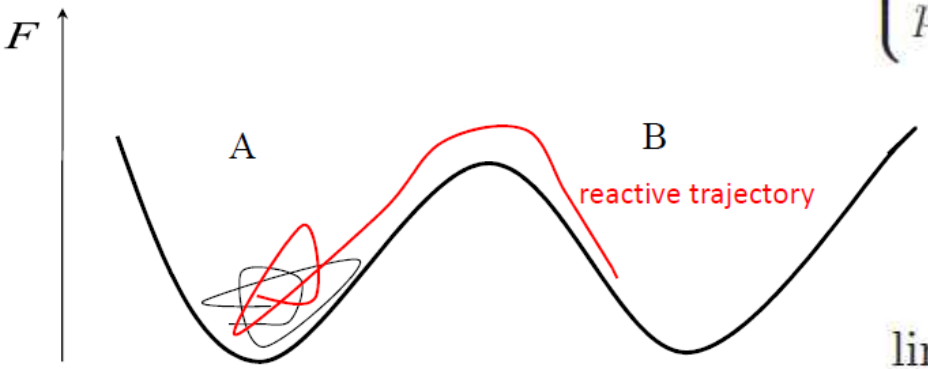


$$\lim_{N \to +\infty} \frac{1}{N} \sum_{n=0}^{N-1} A(q^n, p^n) = \int_{T^*\mathcal{M}} A(q,p)\, d\mu(q,p)$$

The goal is to have the values for transition rates

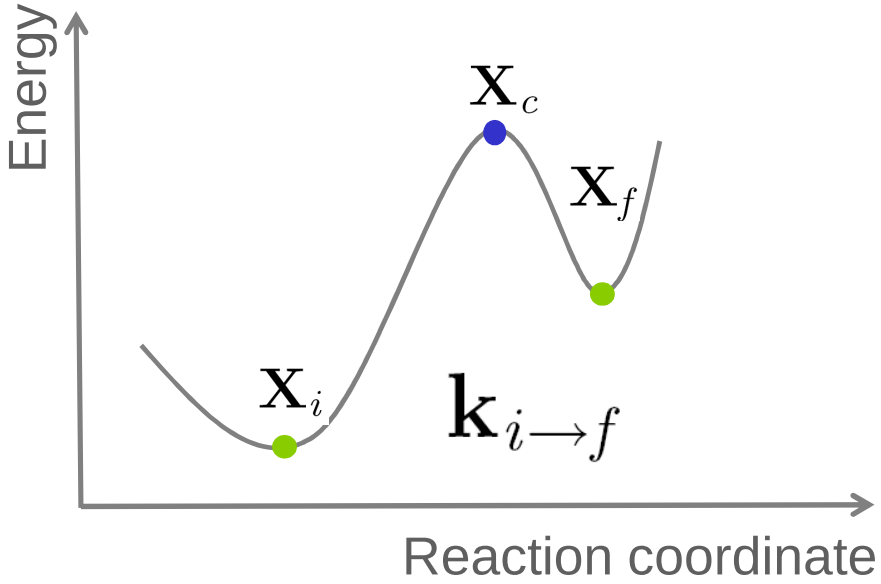


… which can be used in any large scale is time and space simulation:

1. Rate theory
2. AKMC,
3. OKMC,
4. EKMC (JERK, FPKMC)
5. …

$$\mathbf{k}_{i\to f} = k \times e^{-\frac{\mathbf{F}_c - \mathbf{F}_i}{k_B T}} = k e^{\frac{\mathbf{S}_c - \mathbf{S}_i}{k_B}} \times e^{-\frac{\mathbf{E}_c - \mathbf{E}_i}{k_B T}} = \nu_0 \times e^{-\frac{\mathbf{E}_c - \mathbf{E}_i}{k_B T}}$$

**Le but:** trouver sur une surface d'énergie potentielle (« PES »):

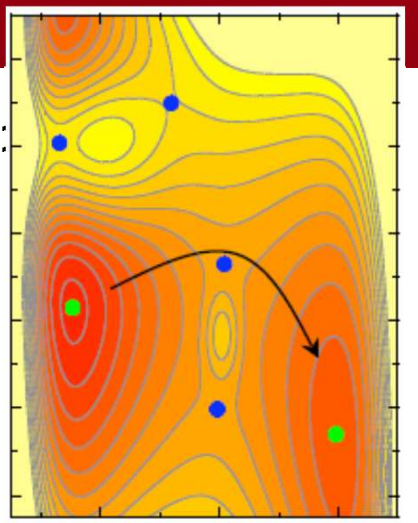

- Les minima **X** : $\mathrm{f}(\mathbf{X}) = 0$ et $\lambda_1 > 0$

  $\mathbf{X} = (\mathrm{q}_1,\ \mathrm{q}_2,\ \ldots, \mathrm{q}_N)$ - la configuration

  $\mathrm{f}(\mathbf{X}) = -\nabla E(\mathbf{X})$ - le gradient

  $\mathbf{H}(\mathbf{X}) = \left\| \dfrac{\partial^2 E}{\partial q_{i\alpha} \partial q_{j\beta}} \right\|$ - le Hessien et son spectre

  $\lambda_1 \leq \lambda_2 \leq \ldots \leq \lambda_{3N}$

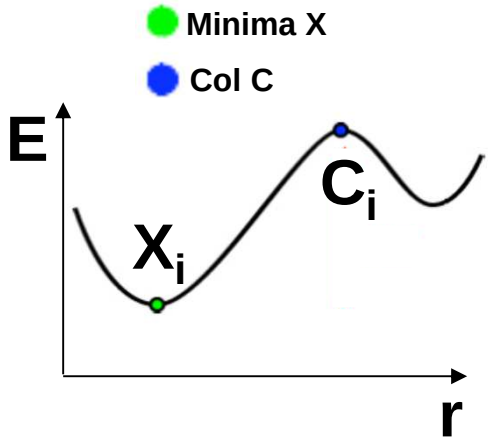


- Les points de cols **C:** $\mathrm{f}(\mathrm{C}) = 0$ et $\lambda_1 < 0$

Dans la suite nous ne faisons pas la différence entre les points de col de 1er, 2ème … ordre

- **$X_I$ et $X_F$ sont connues** :
  - Application directe du principe de Hamilton: minimisation de l'action de la trajectoire qui lie les deux bassins

$$\delta S = 0$$

$$S = \int_0^t L\left(\mathbf{X}(\tau), \dot{\mathbf{X}}(\tau)\right) d\tau \approx \frac{t}{N+1} \sum_{J=0}^{N} L_J\left(\mathbf{X}_J, \dot{\mathbf{X}}_J\right)$$

$$\mathbf{X}(0) = \mathbf{X}_I$$

$$\mathbf{X}(t) = \mathbf{X}_F$$

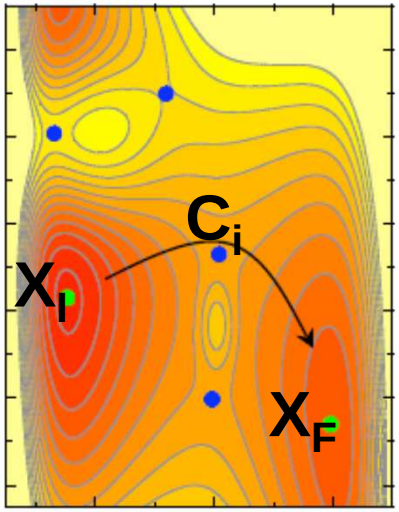


  - Exemples:
    - relaxation sous contraintes: Bennet, drag

$$S = \sum_J E(\mathbf{X}_J) \qquad (\mathbf{X}_J - \mathbf{X}_{CM})\left(\mathbf{X}^F - \mathbf{X}^I\right) = 0$$

    - les méthodes de chaines (Ulitsky-Elber, NEB, CI-NEB etc)

$$S = \sum_J E(\mathbf{X}_J) + \frac{1}{2} k \sum_J \left( \| \mathbf{X}_{J+1} - \mathbf{X}_J \|^2 - \| \mathbf{X}_J - \mathbf{X}_{J-1} \|^2 \right)$$

    - Dynamique moléculaire par Action (ADM)

$$S = \frac{t}{N+1} \sum_{J=0}^{N} L_J\left(\mathbf{X}_J, \dot{\mathbf{X}}_J\right) \qquad L_J\left(\mathbf{X}_J, \dot{\mathbf{X}}_J\right) \approx L_J\left(\mathbf{X}_J, \mathbf{X}_{J\pm1}\right)$$

# The Activation Relaxation Technique (ART)

**A method to explore a potential energy surface: search for saddle points and local minima**

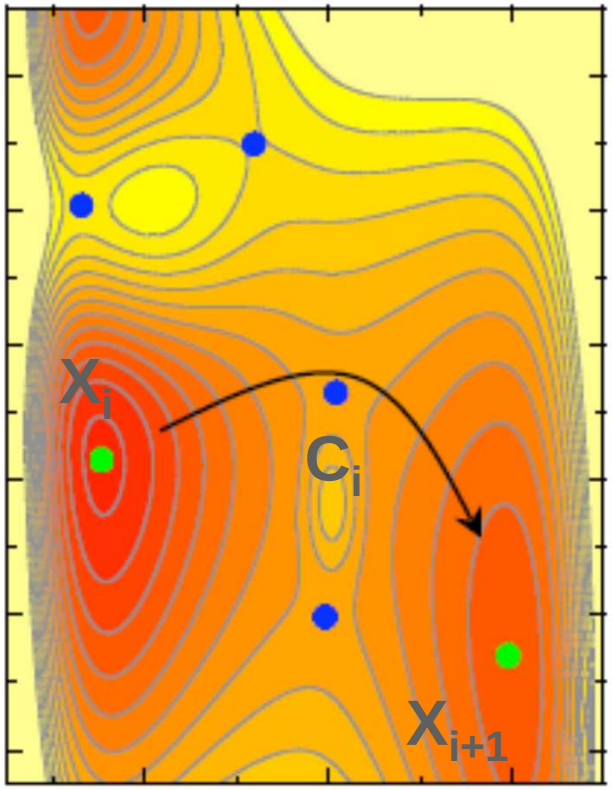


A. Barkema, N. Mousseau PRL (1998) ; Phys. Rev. B (2000)
E. Cances, F. Legoll, M.C. Marinica, F. Willaime, J. Chem. Phys (2009)
M.C. Marinica, F. Willaime, N. Mousseau, Phys. Rev. B, (2011)

- **$X_I$ is known** the others minima $\{X_i\}$ and the saddle points $\{C_i\}$ must be revealed by the method:
  - 0 K method, local information; partial Hessian
  - Fast, adapted for defects
  - Tested for Fe, Cu, Zr, W, Si, SiC

Lanczos method: **ART**

- Hessian is required only in the j-dimension space j << 3N (j=15-30)
- diagonalization of the trigonal jXj matrix

G. T. Barkema and N. Mousseau PRL (1998) ; PRB (2000)

Update 2015:

- **GAD** (W. E)
- **RAT** (R. Smith)
- **String M** (E. van Eijden)

The central point of the method: the evaluation of the lowest eigenvalue and the correspondig eigenvector $\lambda_1$ and $\mathbf{v_1}$

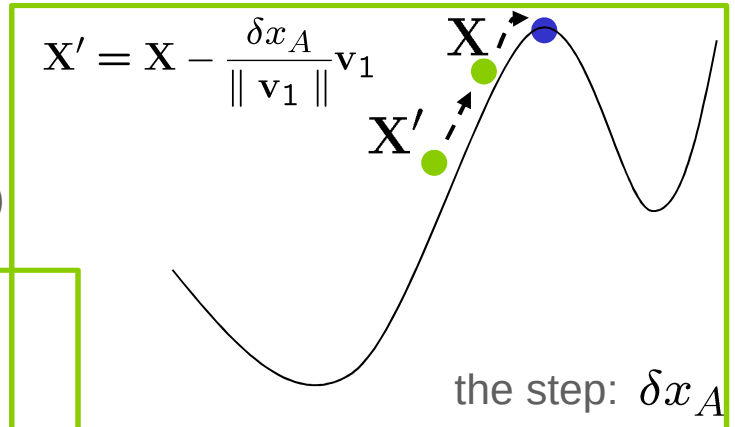


minimization in the hyperplane

*Definition* of the inflexion point:

$\lambda_1 < - |\lambda_c|$

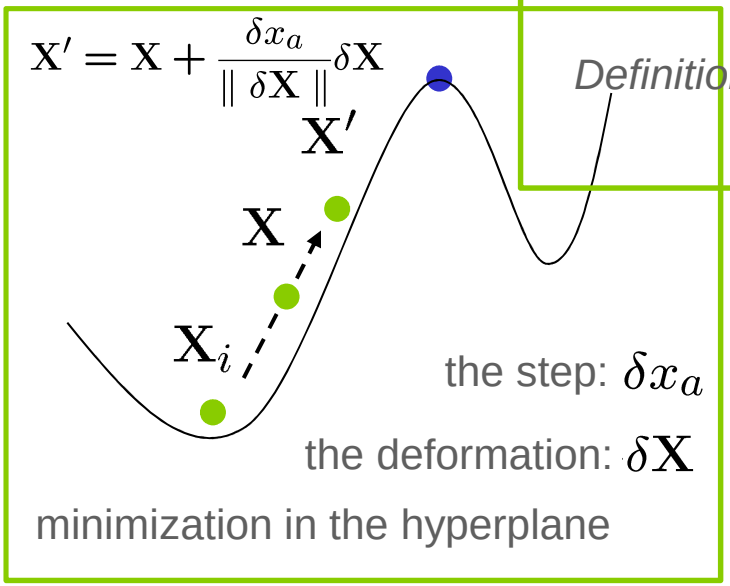


minimization in the hyperplane

Rayleigh-Ritz **HEF**

- CG / L-BFGS optimization using the Rayleigh-Ritz criterion

D. Wales and J. Murno PRB (1998)

finite differences: **DIMER**

- the dimer is centered on **X**: **X+ δX** et **X-δX**
- $\mathbf{v_1}$ (orientation of the dimer), $\lambda_1$ (is estimated from the energy and the gradient)

Henkelman and Jonsson JCP, (1999)

$\lambda_1 \left[\mathbf{T}_j\right] \rightarrow \lambda_1 \left[\mathbf{H}\right]$

**En général j=15-40**

$$(\mathbf{u}_0, \mathbf{u}_1, \ldots, \mathbf{u}_{l-1})$$

$$\mathbf{T}_l = \begin{pmatrix} a_0 & b_1 & 0 & \cdots & 0 \\ b_1 & a_1 & b_2 & \cdots & 0 \\ 0 & b_2 & a_2 & \cdots & 0 \\ 0 & \ddots & \ddots & \cdots & 0 \\ 0 & & b_{l-2} & a_{l-2} & b_{l-1} \\ 0 & & 0 & b_{l-1} & a_{l-1} \end{pmatrix}$$

$$\mathbf{H}\mathbf{u}_0 = a_0\mathbf{u}_0 + b_1\mathbf{u}_1$$

$$\mathbf{H}\mathbf{u}_1 = a_1\mathbf{u}_1 + b_1'\mathbf{u}_0 + b_2\mathbf{u}_2$$

$$\mathbf{u}_1 \cdot (\mathbf{H}\mathbf{u}_0) = \mathbf{u}_0 \cdot (\mathbf{H}\mathbf{u}_1)$$

$$\cdots$$

$$\mathbf{H}\mathbf{u}_k = a_k\mathbf{u}_k + b_k\mathbf{u}_{k-1} + b_{k+1}\mathbf{u}_{k+1}$$

$$\cdots$$

$$\mathbf{H}\mathbf{u}_{l-1} = a_{l-1}\mathbf{u}_{l-1} + b_{l-1}\mathbf{u}_{l-2}$$

$$H_{i\alpha,j\beta}[\mathbf{q}_0] = \frac{\partial^2 E[\mathbf{q}_0]}{\partial q_{i\alpha}\partial q_{j\beta}}$$

$$\mathbf{H}\left[\mathbf{q}_0\right]\mathbf{u} = -\frac{\mathbf{f}\left(\mathbf{q}_0 + \delta_L\mathbf{u}\right) - \mathbf{f}\left(\mathbf{q}_0\right)}{\delta_L}$$

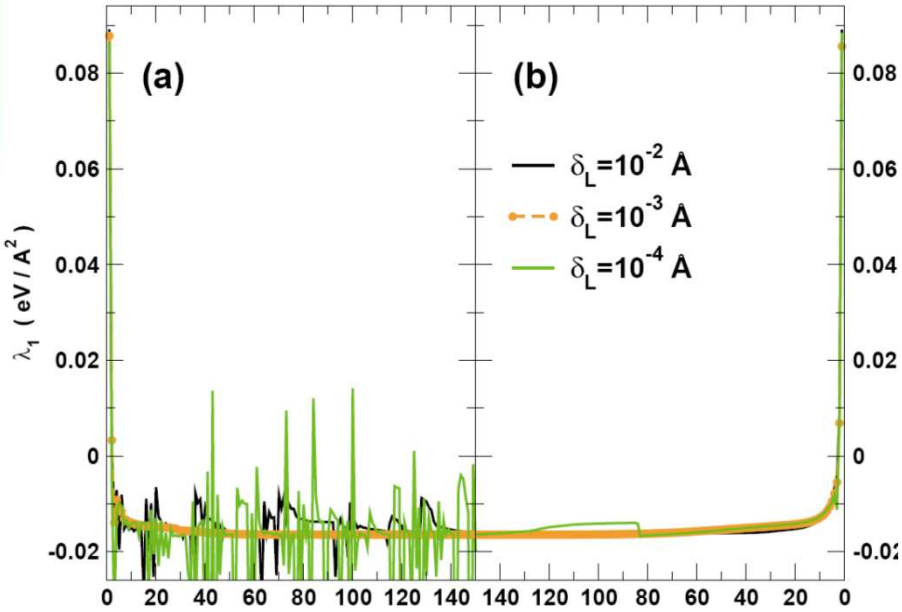


$$\mathbf{H}\left[\mathbf{q}_0\right]\mathbf{u} = -\frac{\mathbf{f}\left(\mathbf{q}_0 + \delta_L\mathbf{u}\right) - \mathbf{f}\left(\mathbf{q}_0 - \delta_L\mathbf{u}\right)}{2\delta_L}$$

we do not need entire H: only in the Krylov-Lanczos basis - dimension j

diagonalisation of trigonal jXj matrix

1. The parameters which must be managed
   - The Lanczos step of the numerical derivative.
   - Size of the Lanczos basis

# The Activation Relaxation Technique (ART)

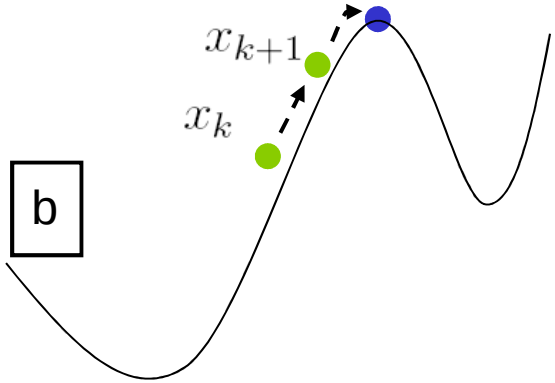


$$x_{k+1} = x_k - \frac{\mu_a}{\sqrt{k}} v_1(x_k) - \mu_t \Pi_{v_1(x_k)^\perp} \nabla f(x_k)$$

$$x_{k+1} = x_k - \frac{(\nabla f(x_k), v_1(x_k))}{\min(\lambda_1(x_k), -\lambda_c)} v_1(x_k) - \mu_t \Pi_{v_1(x_k)^\perp} \nabla f(x_k)$$

$$\Pi_{v_1(x_k)^\perp} = I - (v_1(x_k), \cdot) v_1(x_k)$$

$$x_{k+1} = x_k - \frac{\delta x_A}{\| \mathbf{v_1} \|} v_1(x_k)$$

$$\delta x_A = \frac{\mu_a}{\sqrt{k}}$$

$$\delta x_A = \frac{(\nabla f(x_k), v_1(x_k))}{\min(\lambda_1(x_k), -\lambda_c)}$$

activation step $\mu_a$

The numbers of distinct minima

| | | |
|---|---|---|
| 0.05 | 1579 | 1 |
| 0.10 | 965 | 2 |
| 0.20 | 553 | 2 |
| 0.40 | 404 | 3 |
| 0.60 | 382 | 4 |
| 0.80 | 424 | 4 |
| 1.00 | 505 | 4 |

# The Activation Relaxation Technique (ART)

$\tilde{\lambda}_1(x_k)$ and $\tilde{v}_1(x_k)$ are approximations of $\lambda_1(x_k)$ and $v_1(x_k)$

$$\tilde{v}_1(x_k) = v_1(x_k) + \alpha_k, \quad \tilde{\lambda}_1(x_k) = \frac{\lambda_1(x_k)}{1+\beta_k}, \quad |\alpha_k| \ll 1 \text{ and } |\beta_k| \ll 1$$

$$|x_{k+1} - x_*| \leq \gamma |x_k - x_*| + O(|x_k - x_*|^2) + O(|x_k - x_*|\,|\alpha_k|) + O(|x_k - x_*|\,|\beta_k|),$$

algorithm locally converges, and the convergence speed is at least linear.

| number of defects | | SIA | | VAC | |
|---|---|---|---|---|---|
| | | ART$n^{44}$ | This work | ART$n^{44}$ | This work |
| 1 | $\langle f \rangle$ | 462 | 298 | 780 | 291 |
| | $\eta$ | 4.6 | 4.7 | 1.8 | 7.9 |
| 2 | $\langle f \rangle$ | 548 | 328 | 705 | 323 |
| | $\eta$ | 4.2 | 4.4 | 2.6 | 7.1 |
| 3 | $\langle f \rangle$ | 691 | 320 | 667 | 321 |
| | $\eta$ | 2.6 | 4.4 | 2.8 | 7.4 |

# Application: di-SIA iron

- many non-parallel configurations between the $I_2^{<110>}$ et $I_2^{<111>}$

- quasi-continuum of states between 0.42 eV and 0.83 eV (dissociation energy of the di-interstitiel)

- beyond the bonding energy two separated SIA

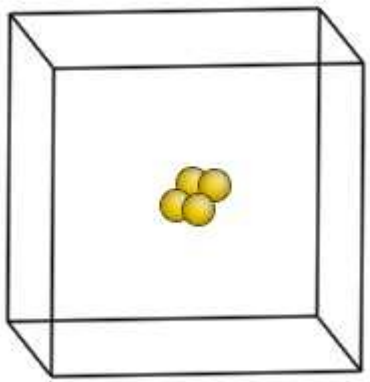

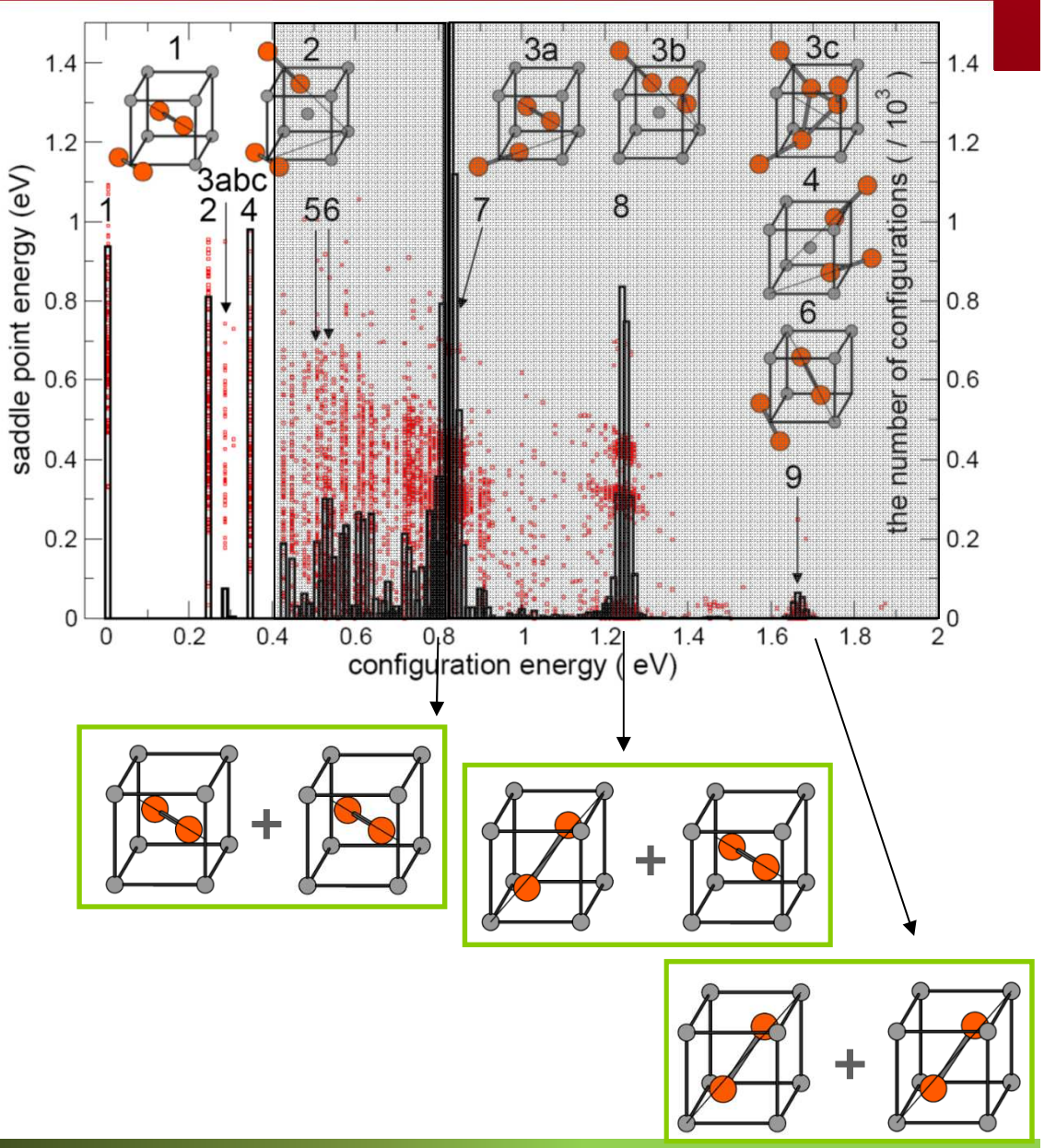

Find the absolut minimum of an energy landscape

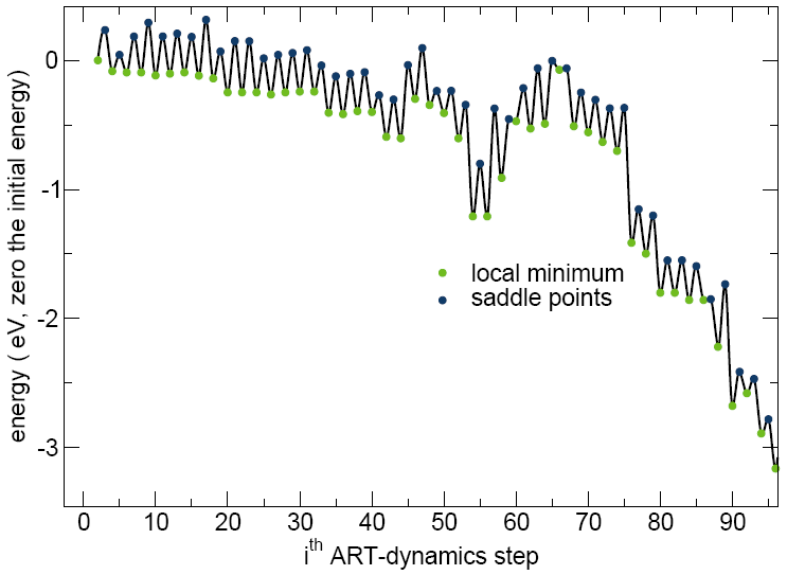


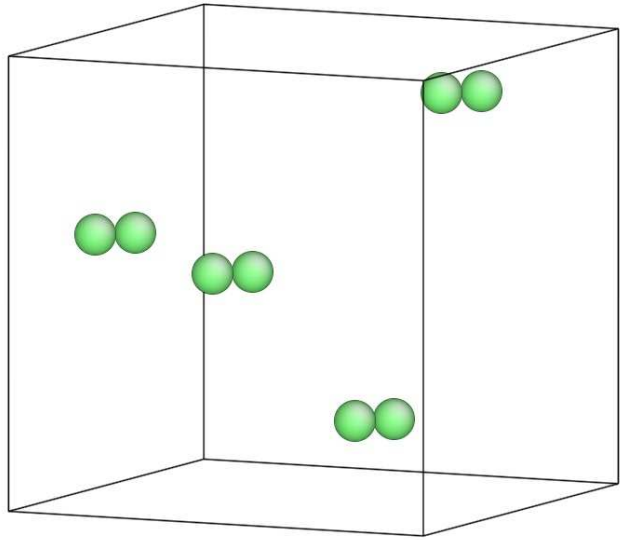

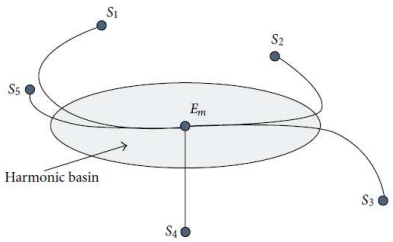


## Kinetic ART

**N. Mousseau et al., Journal of Atomic, Molecular, and Optical Physics. 2012, 1–14 (2012).**

1. **ART biblio:**

   a. **ART :**
      - ✓ G. T. Barkema, N. Mousseau, ***I***Phys. Rev. Lett. **81,** 1865 (1998).

   b. **ART nouveau :**
      - ✓ N. Mousseau, G. T. Barkema**,** Phys. Rev. B **61**, 1898-1906 (2000).
      - ✓ A. Barkema, N. Mousseau Phys. Rev. Lett. (1998)
      - ✓ E. Cances, F. Legoll, M.C. Marinica, F. Willaime, J. Chem. Phys (2009)
      - ✓ M.C. Marinica, F. Willaime, N. Mousseau, Phys. Rev. B, (2011)

2. **Sources ARTn (C et F90, also interfaced with SIESTA, PWSCF)**

http://www.phys.umontreal.ca/ mousseau/index.php?n=Main.Logiciels

**Ou**

**GOOGLE: ART Mousseau**

2. **kART, under request**

# Elementary defects induced by irradiation

Materials under irradiation for the nuclear industry (e. g. high fluxes of neutrons)

⇨ Defect or Defect clusters

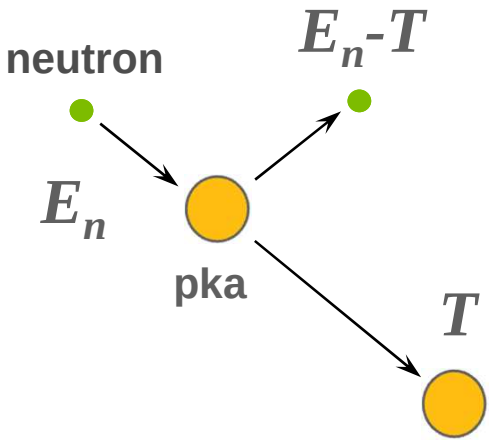


pka = primary knocked atom
T = kinetic energy transferred to the pka

Number of Frenkel pairs :

$n \approx \alpha T / (2.E_d)$

$T>>E_d$ => displacement cascade

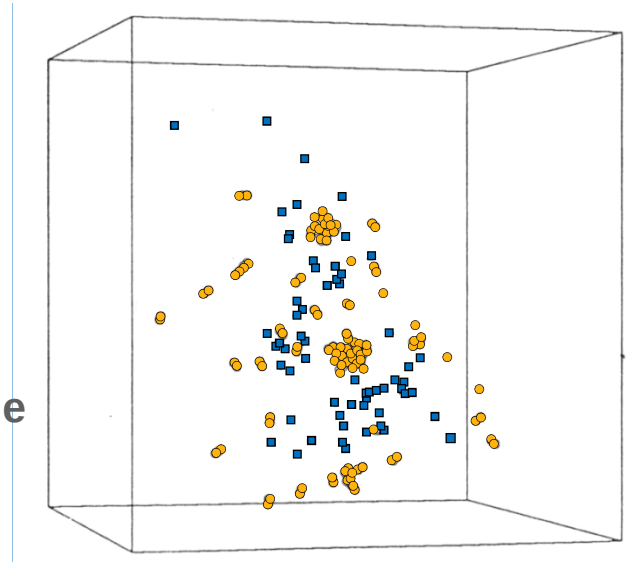


- Isolated self-interstitials
- Isolated vacancies.
- Interstitial clusters.
- Vacancies clusters.

+

- atomic mixing: *( ≈10Resplacements /displacement )*

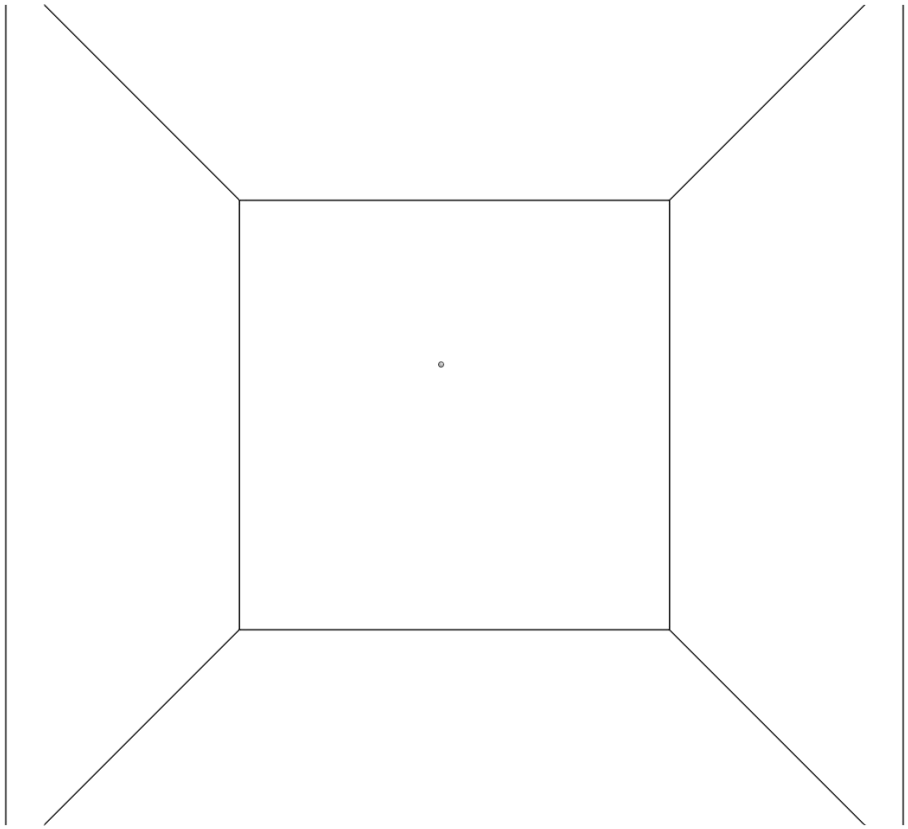

Molecular Dynamics simulations, 80 keV, 3 $10^6$ atoms, 10 ps
L. Van Brutzel (CEA/Saclay, France)

# Elementary defects induced by irradiation

## ❑ Annihilation (recombination)

- system tend to recover the ground state (bulk state)

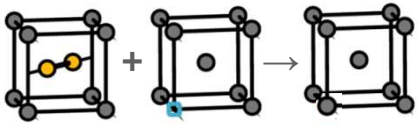

I + V → bulk (atom on a lattice site)

## ❑ Clustering (agglomeration)

- vacancy : $V_n + V_m \rightarrow V_{n+m}$

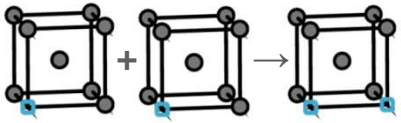

V + V → $V_2$

- interstitial : $I_n + I_m \rightarrow I_{n+m}$

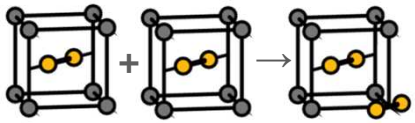

I + I → $I_2$

- annihilation: $I_n + V_m \rightarrow I_{n-m}$ ($V_{m-n}$)

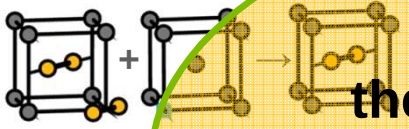

$I_2$ + V → I

## ❑ Elimination on sinks

- Dislocation lines (network & loops),
- Grain-boundaries
- Free surfaces, voids, bubbles.

**Common feature: thermally activated atom jumps ; slow evolution of the point defect population**

# MORPHOLOGY OF DEFECT CLUSTERS IN METALS UNDER IRRADIATION

n=1 — 10 — 100-10 000 # defects in cluster

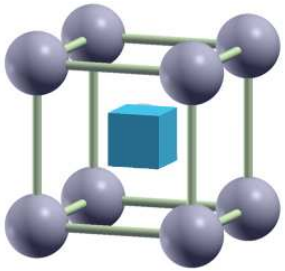

**3D**

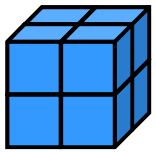

voids

**3D**

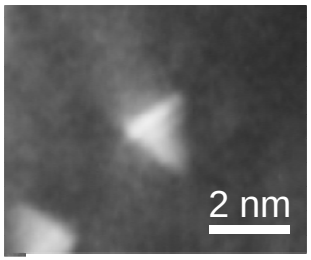


SFT

**2D**

loops

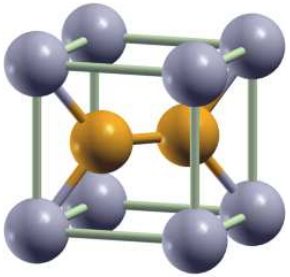

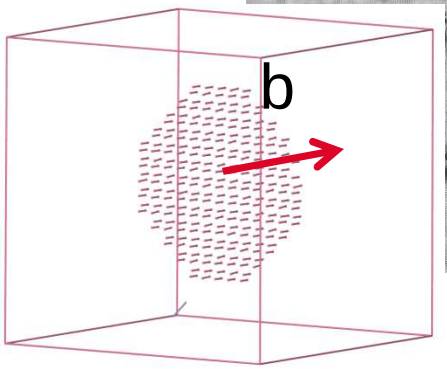


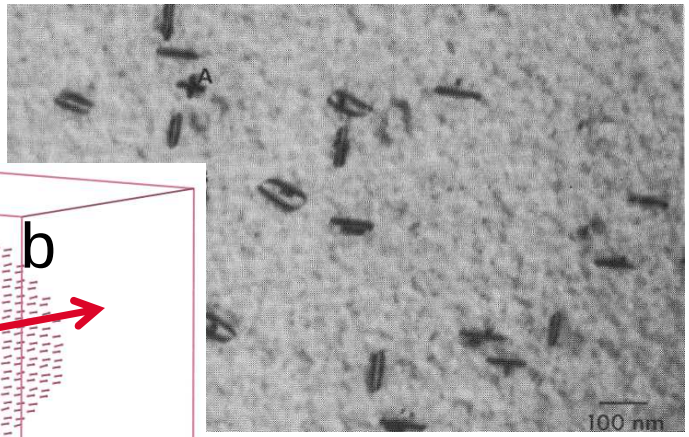


**2D**

# MORPHOLOGY OF DEFECT CLUSTERS IN METALS UNDER IRRADIATION

n=1 — 10 — 100-10 000 # defects in cluster

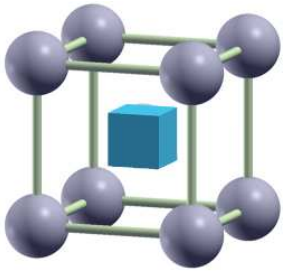

3D

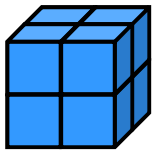

voids

3D

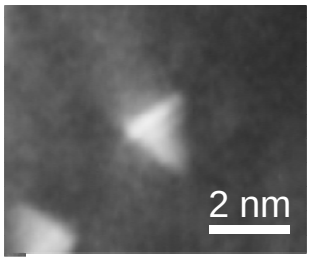


SFT

2D

loops

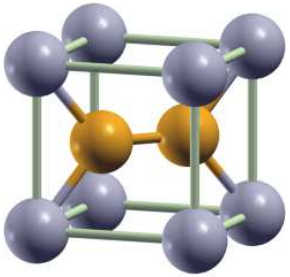

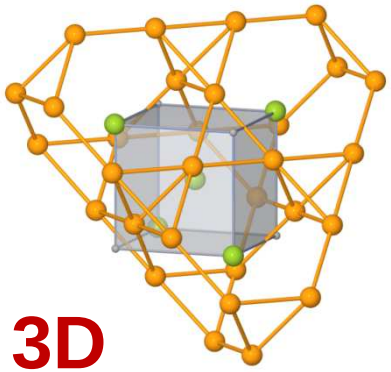

3D

Prediction from atomistic simulations

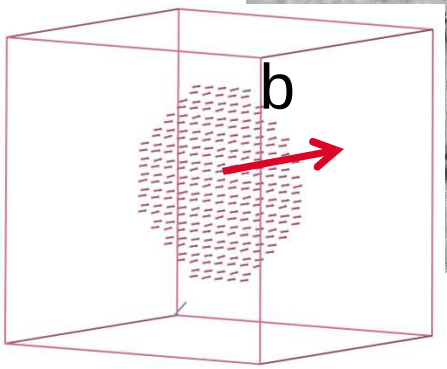


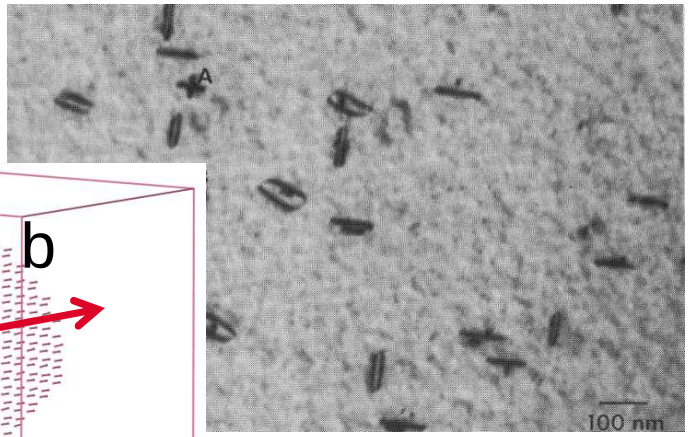


2D

# New type of clusters

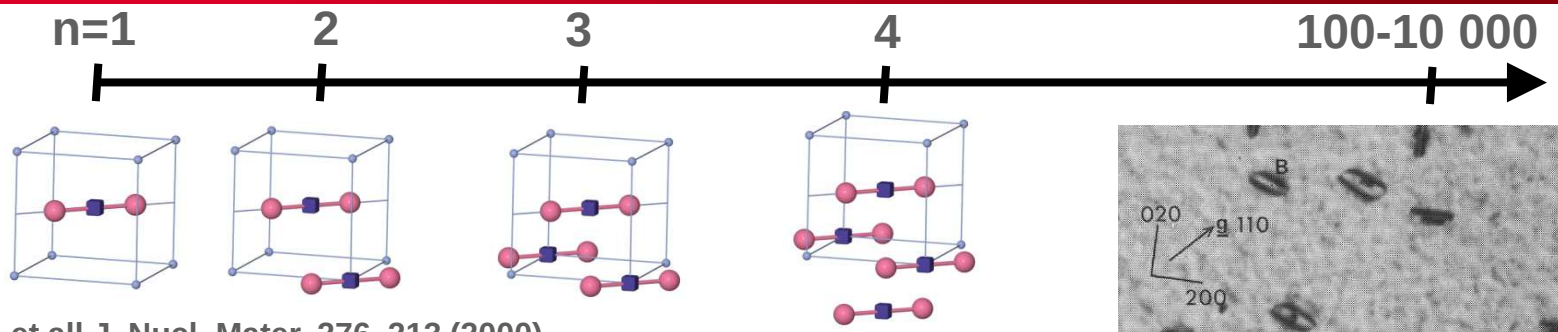


F. Gao et all J. Nucl. Mater. 276, 213 (2000).
C. Domain, C. S. Becquart, Phys. Rev. B 65, 024103 (2001)
C.-C. Fu, F. Willaime, and P. Ordejon, Phys. Rev. Lett. 92, 175503 (2004).

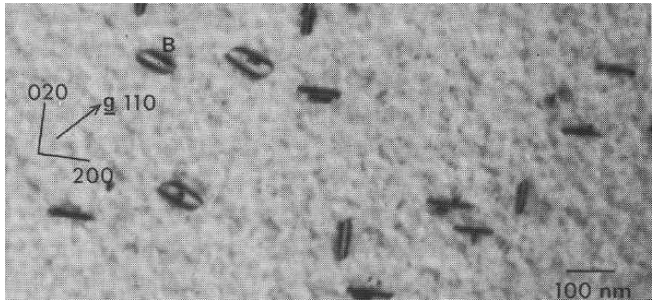


D.A Terentyev et al.
Phys. Rev. Lett.
100, 145503 (2008)

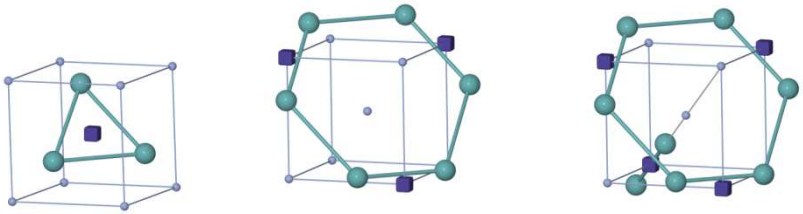

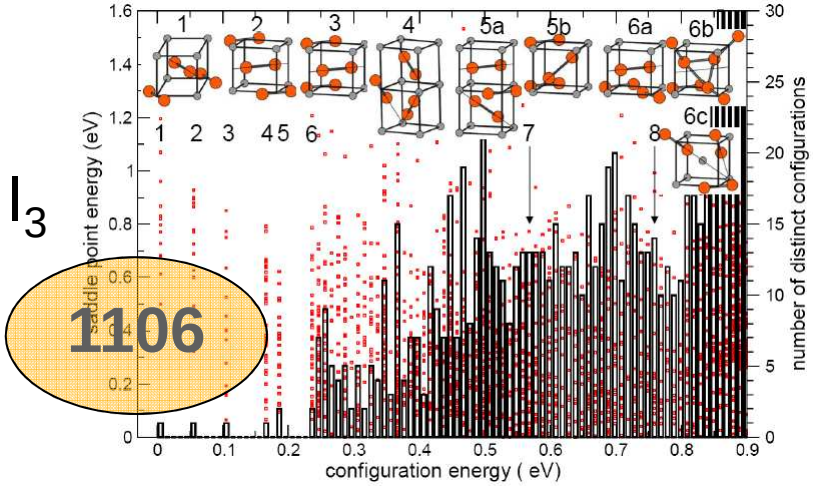


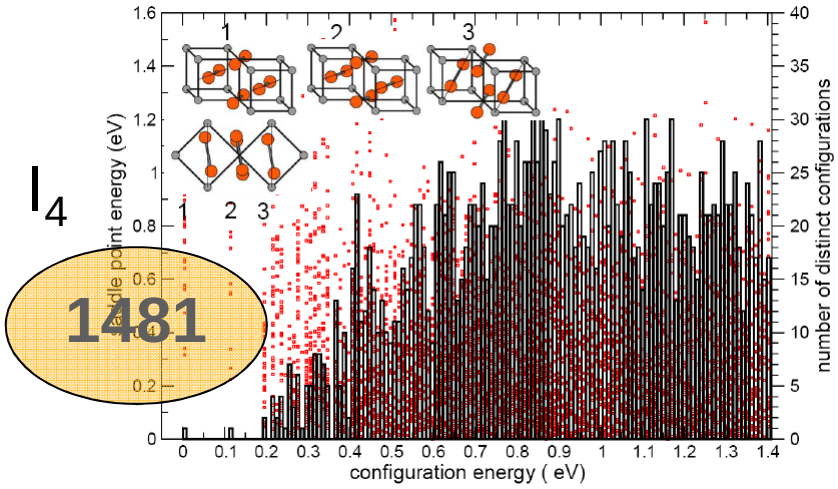


- many non-parallels configurations between $I_3^{<110>}$ and $I_3^{<111>}$
- quasi-continuum of states
- thousands of binding configurations for $I_2$, $I_3$ and $I_4$, respectively.

M.C. Marinica et al PRB 83 (2011) 094119

# Disconectivity graph: archetypal energy landscape

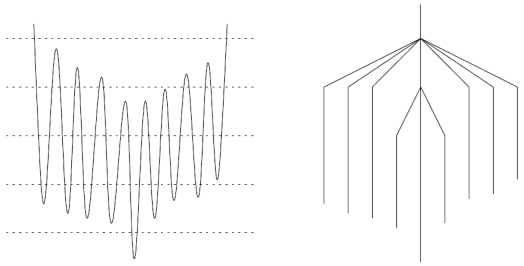

**High downhill barriers, no well defined global minimun**

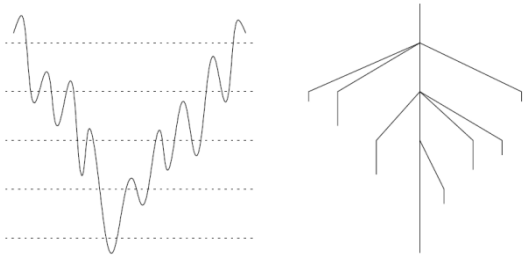

**Low downhill barrires and well defined global minimum**

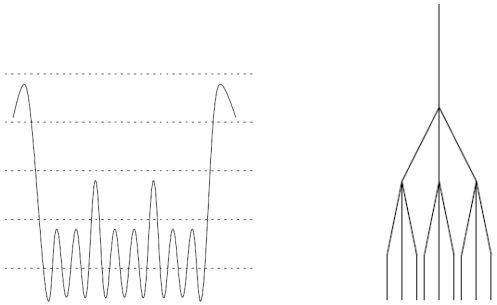

**‘Rough’ landscape, e.g. glasses**


O. M. Becker and M. Karplus, J. Chem. Phys. **106**, 1495 (1997)
D. J. Wales, M. A. Miller, and T. Walsh, Nature **394**, 758 (1998)
D. J. Wales, Energy Landscapes, Cambridge University Press

# Disconnectivity graph: Non-Parallel dumbbells in Fe

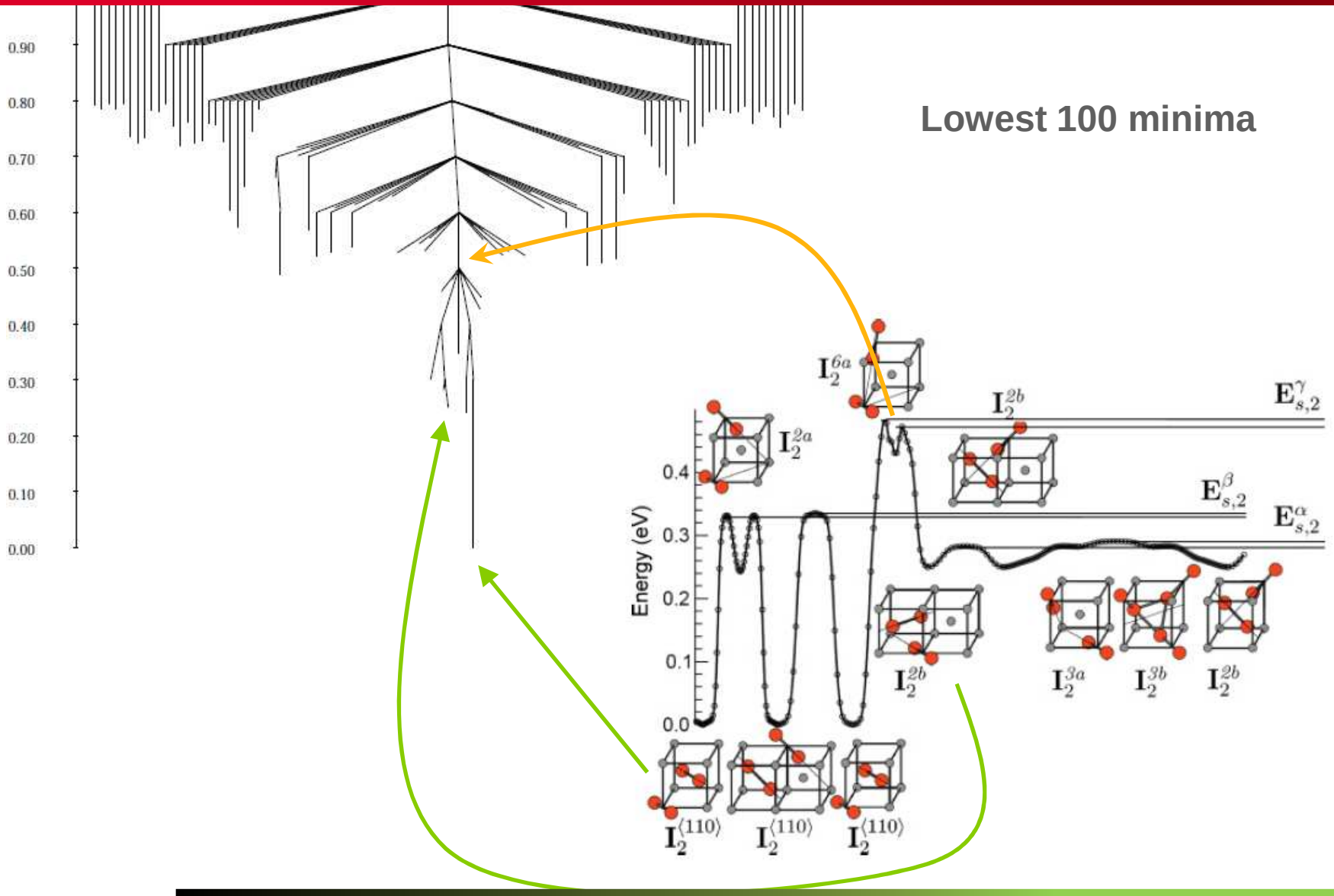

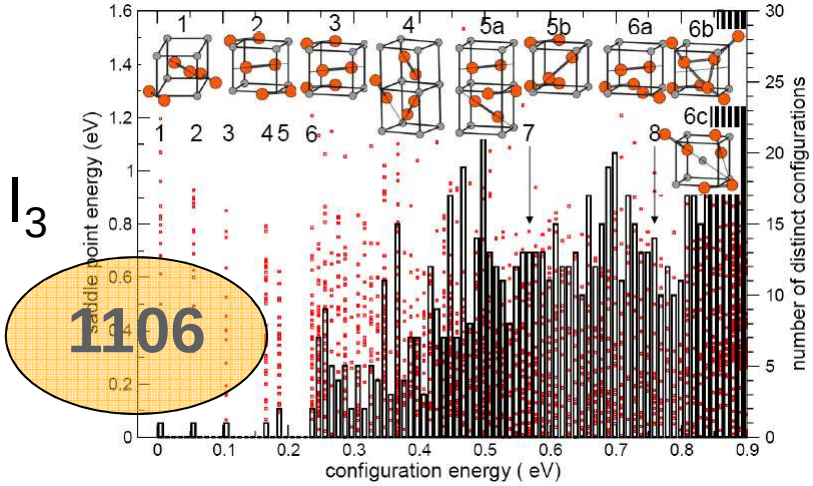
I3
1106
saddle point energy (eV)
number of distinct configurations
configuration energy ( eV)
1 2 3 4 5 6 7 8 6a 6b 6c 5a 5b

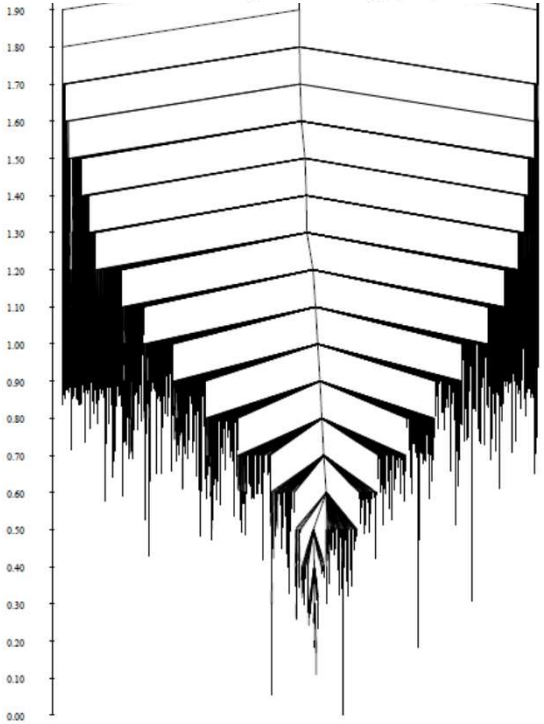

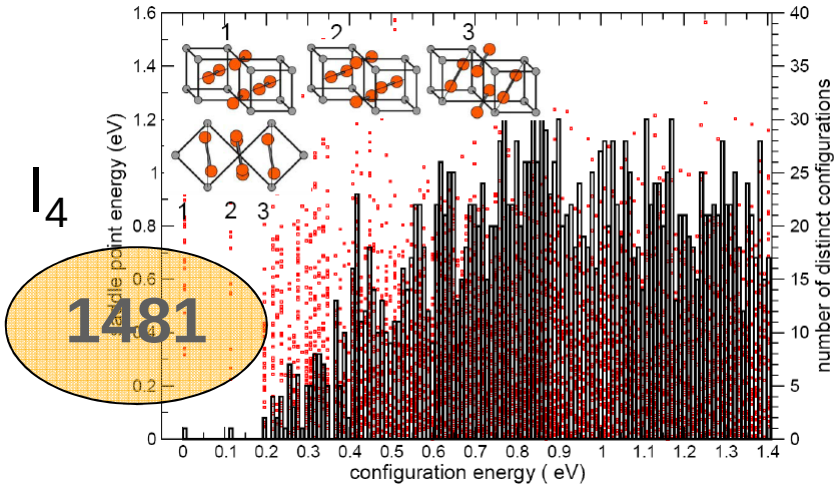
I4
1481
saddle point energy (eV)
number of distinct configurations
configuration energy ( eV)
1 2 3

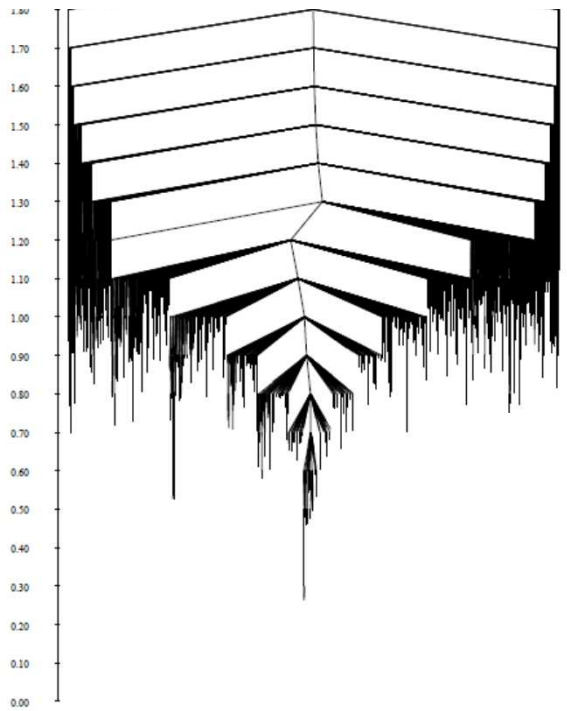

# Non-Parallel dumbbells

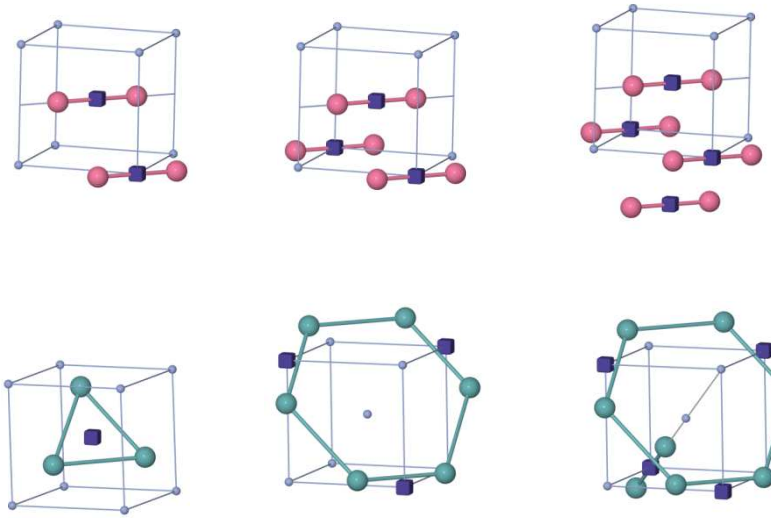

1. **Self-trapped configurations (I4)**
2. **Stabilized at high temperature**

**D.A Terentyev et al Phys. Rev. Lett. 100, 145503 (2008)**

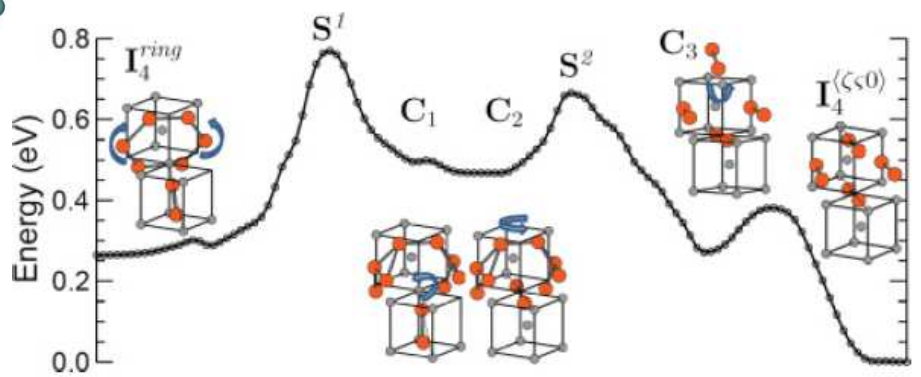


| | $\Delta E_F$ | $\Delta S_F$ | | $\Delta E_F$ | $\Delta S_F$ | | $\Delta E_F$ | $\Delta S_F$ |
|---|---|---|---|---|---|---|---|---|
| EAM | 0.31 | 6.5 | | 0.79 | 10.0 | | 0.25 | 12.9 |
| SIESTA | -0.05 | | | 0.63 | | | 0.47 | |
| VASP | -0.11 | | | -0.06 | | | 0.07 | |

New configurations of I2, I3 and I4 become more stable above resp. 550 K, 920 K and 225K

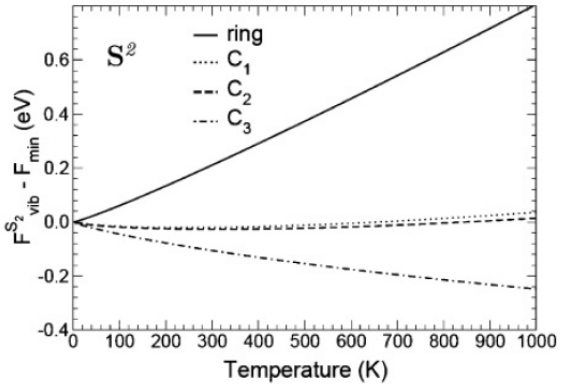

# Origin of the large formation entropy

• For clarity we present a cell with only 128 atoms and

• the atoms where the localization of the mode ($\Sigma_\alpha|\xi_{i\alpha,p}|^2$) is higher than a critical value ( 0.01 $A^2$)

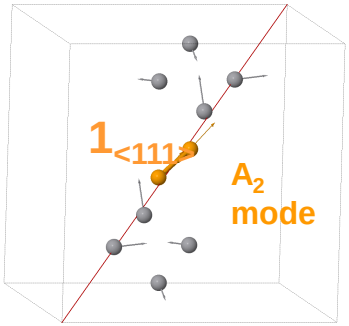


• $\xi_{i\alpha,p}$ is the eigenvector associated to the $i^{th}$ atom in the direction α of the $p^{th}$ mode.

• The orange atoms are the defect atoms and gray atoms are the bulk atoms which fulfil the above localization criterion.

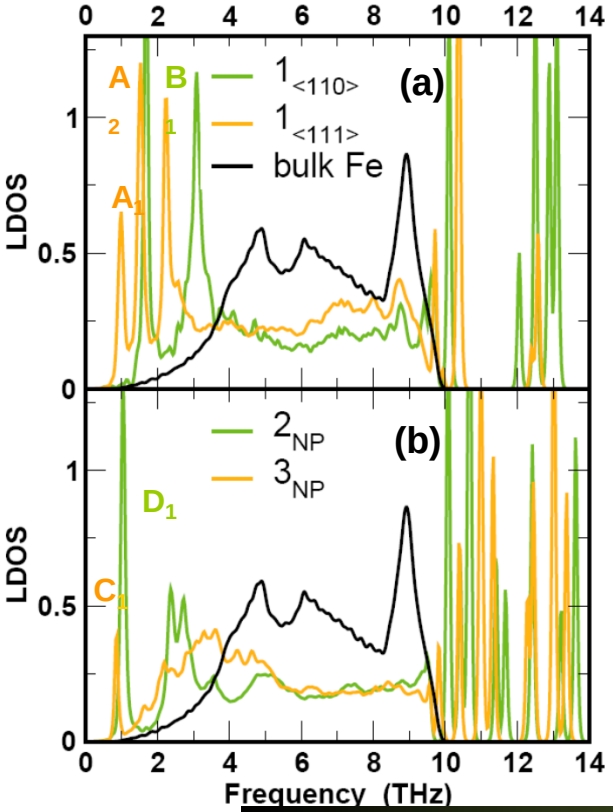


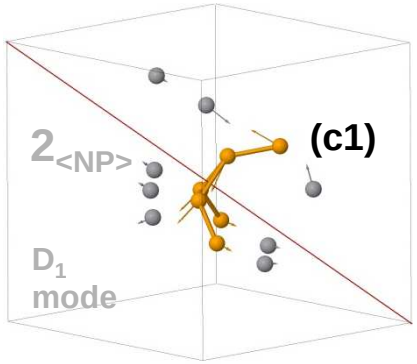


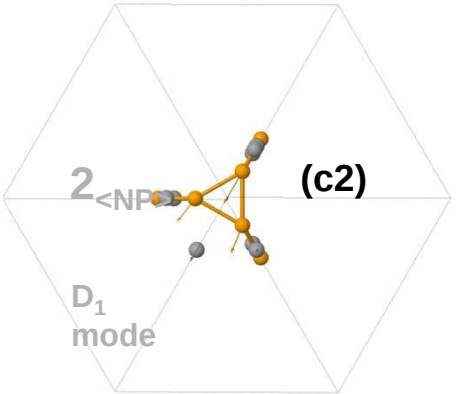


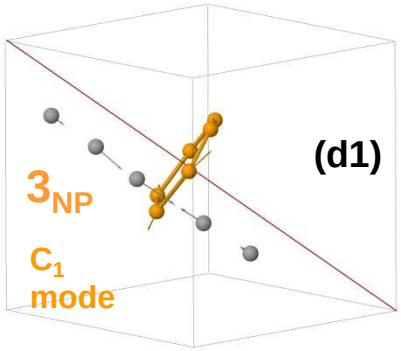


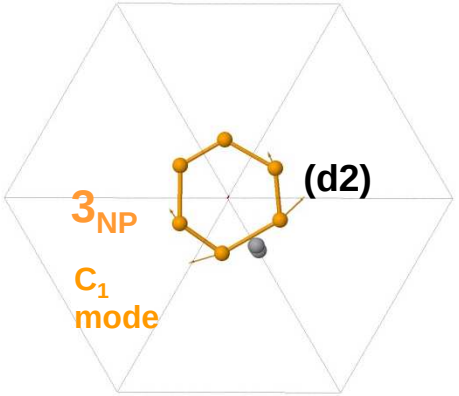

# Application to $I_n$: ART+HA

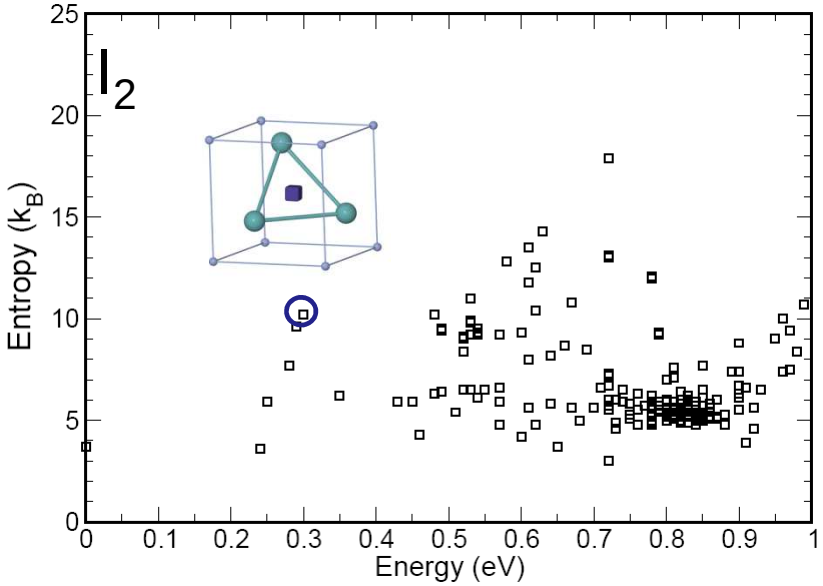


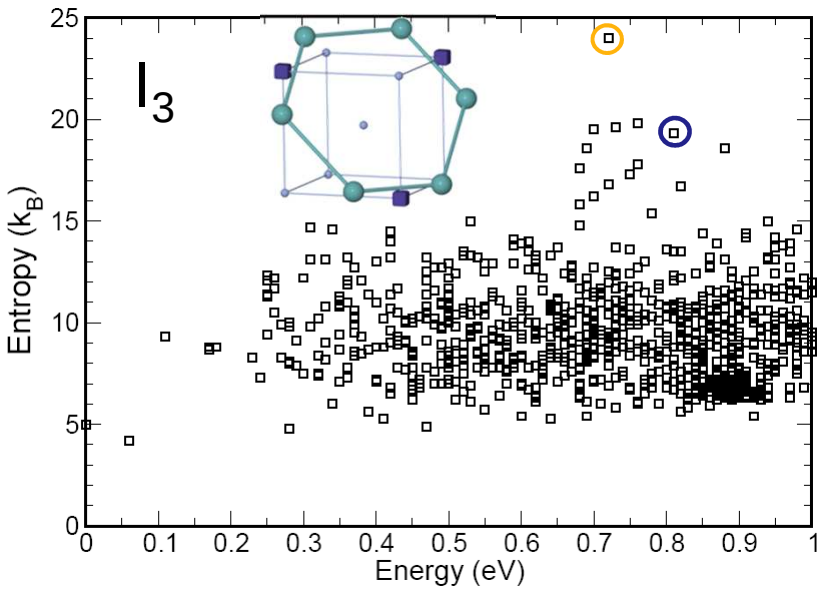


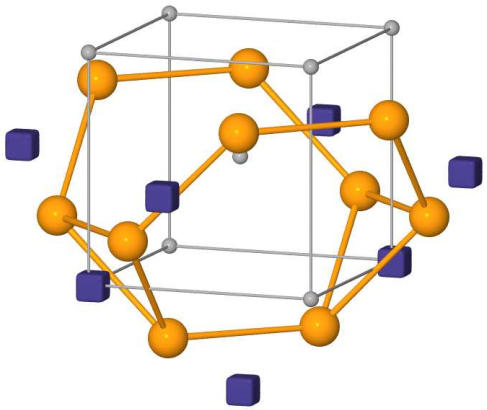

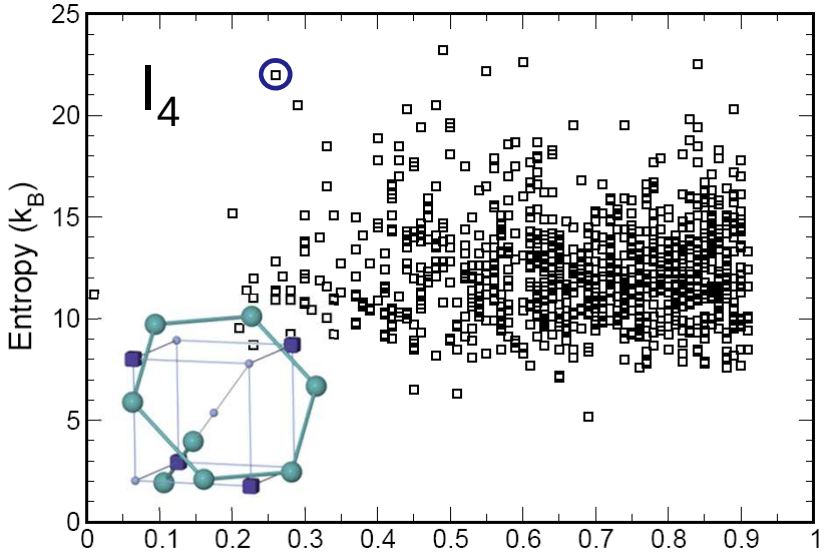

# Building a new type of interstitial clusters

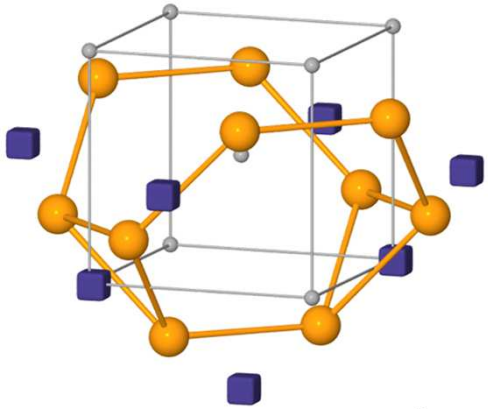

**How to combine the triangle and ring defects ?**

$I_2$

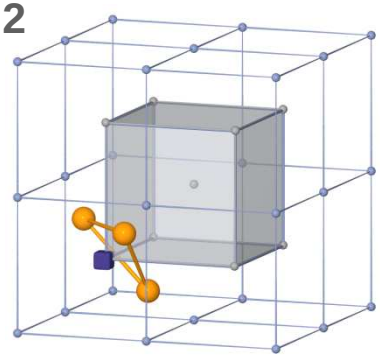

**3i - 1v**

$I_3$

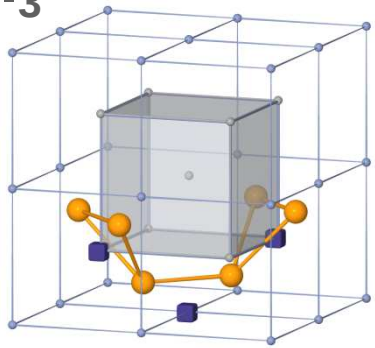

**6i - 3v**

$I_3$

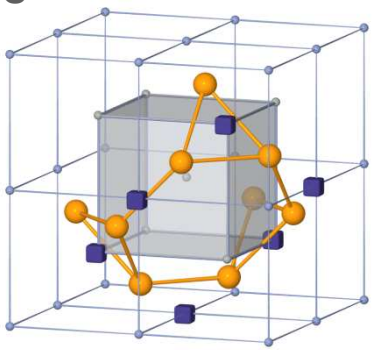

**9i - 6v**

$I_2$

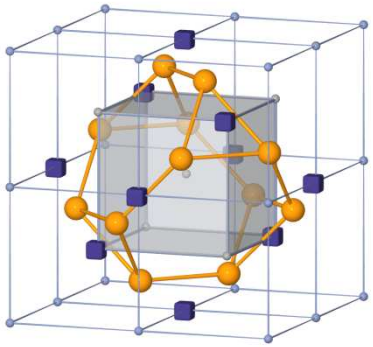

**12i - 10v**

**4 triangles**
**4 rings**

# Di-interstitial

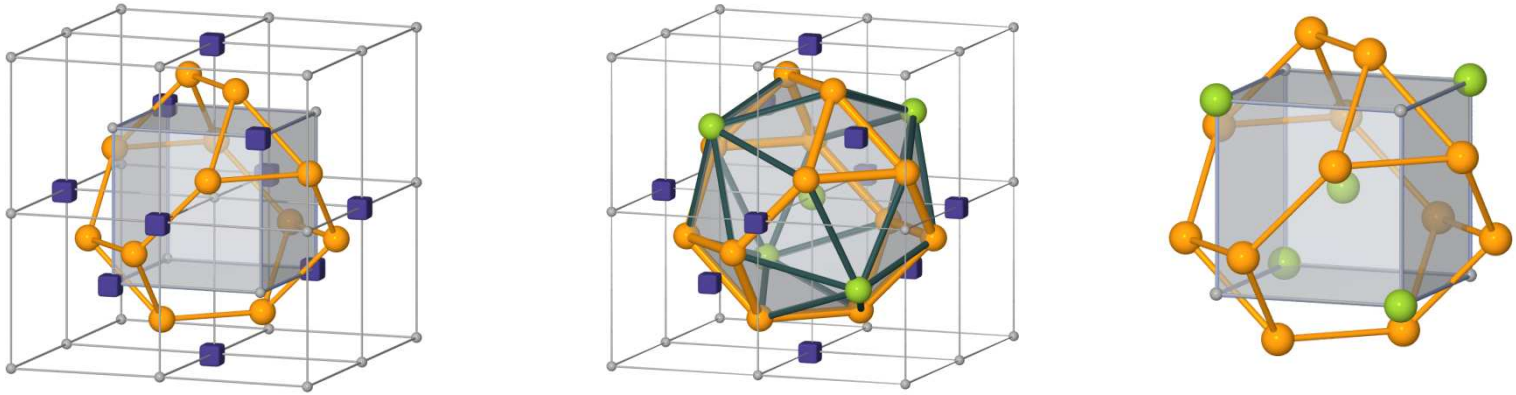

**Z16 Frank-Kasper polyhedra**

1. Low formation energy (ab initio): + 0.71 eV (compared to 110 cluster, 0.12 eV binding energy)
2. Very large antiferromagnetic moment: -33 $\mu_B$ compared to the bulk ! (-8 $\mu_B$ in the case of <110> dumbbell)
3. Small formation volume (ab initio)
4. Large formation entropy (some empirical potential): + 24 $k_B$ (4 $k_B$ in the case of 110)

# Building larger clusters

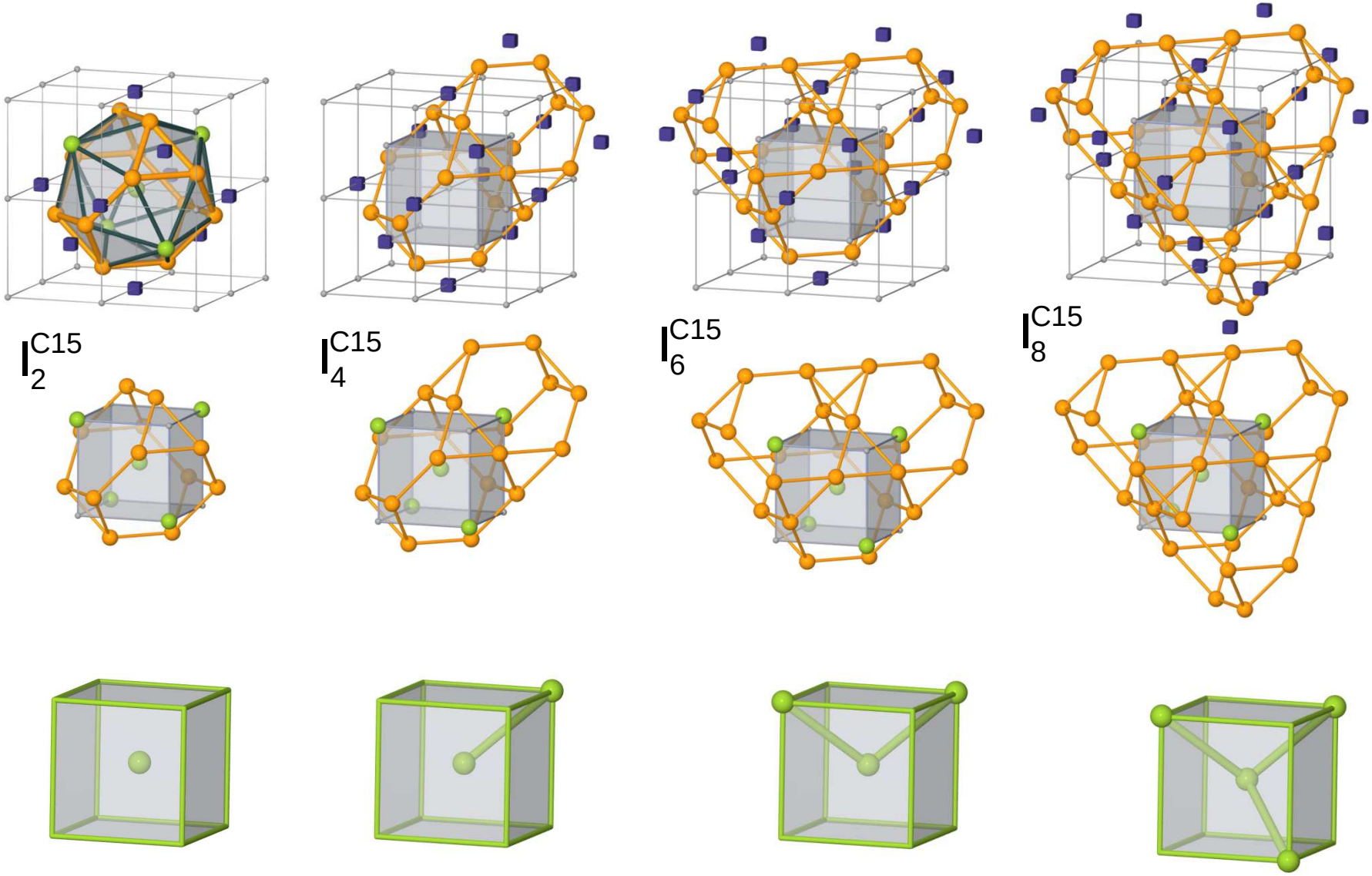

# Identification of the crystal structure: C15 Laves phase

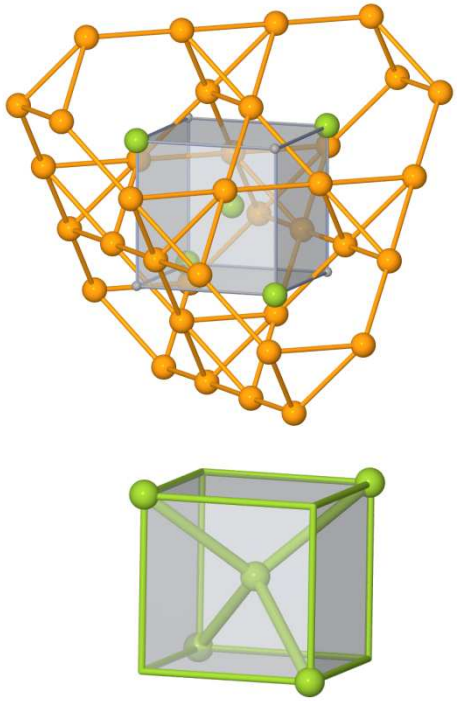

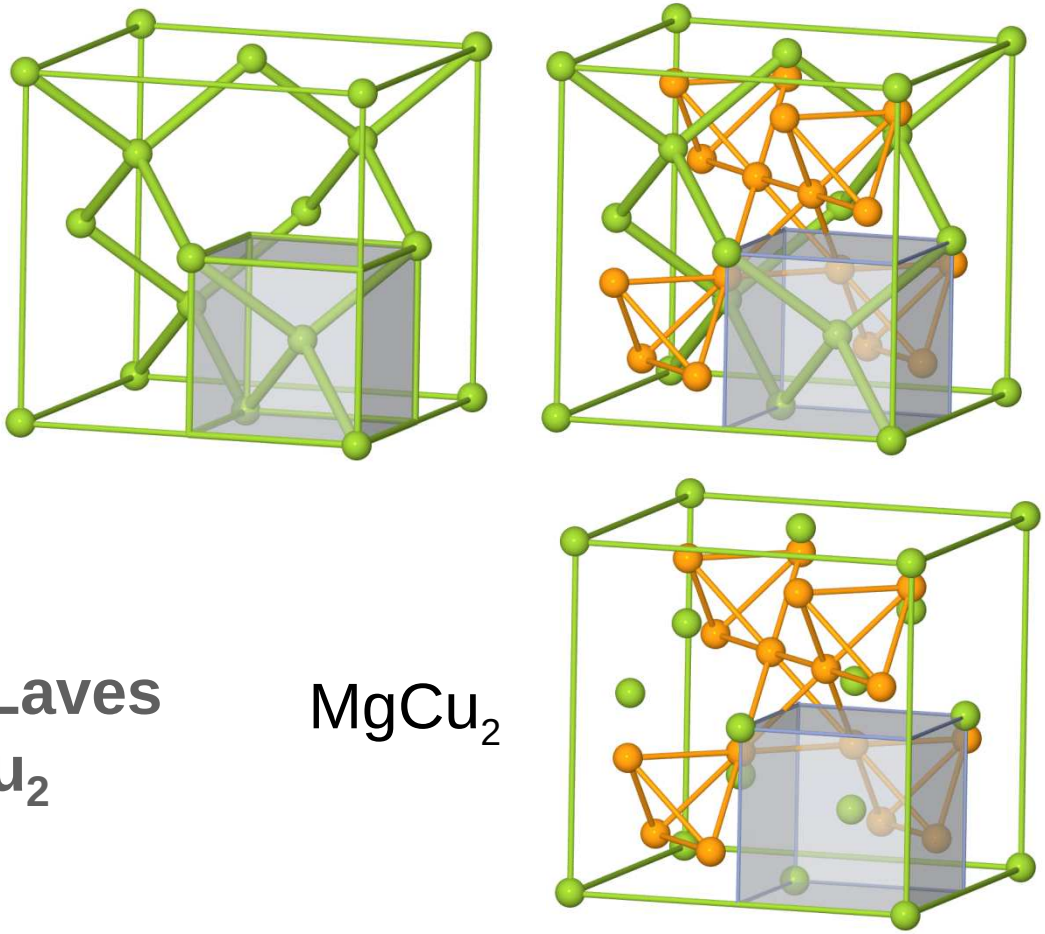

**Cubic Phase of Laves**
**C15 or $MgCu_2$**

$MgCu_2$

# Interstitial clusters in Cubic Phase of Laves C15 or MgCu2

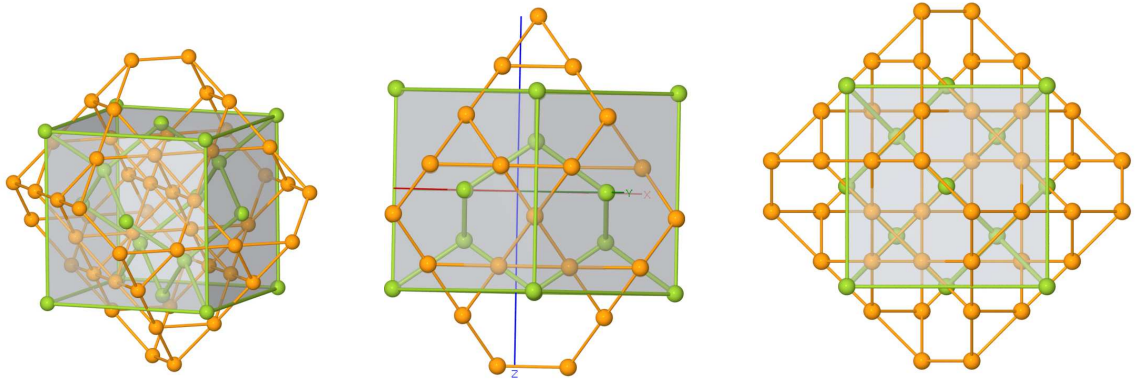

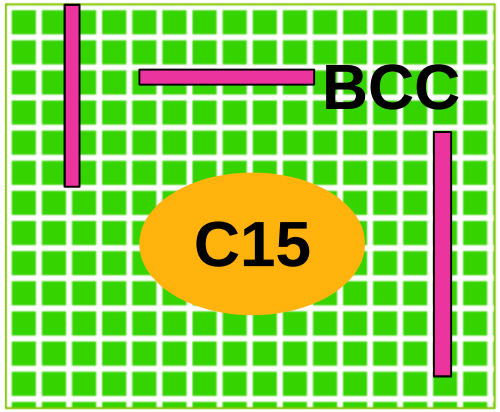


-C15 coherent with the BCC matrix
- C15 have 3D structure as opposed to the 2D structure of dislocation loops

M.C. Marinica, F. Willaime, J.-P. Crocombette, Phys. Rev. Lett. (2012)

# TECHNICALITIES

Density Functional Theory

- *ab initio* electronic structure calculations
- PWSCF (Quantum Espresso) code
- 250 to 432 atom supercells

Formation energies of self-interstitial clusters (in all bcc metals)

Empirical interatomic potential for Fe

- Embedded Atom Method type
- Parameters fitted to bulk and point defect properties (DFT database)

Cascade simulations
(Molecular Dynamics)

Energy landscape of interstitial clusters
(Activation Relaxation Technique)

Representation
(Disconnectivity graph)

# Characteristics of C15 clusters

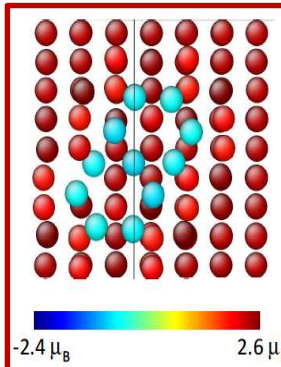


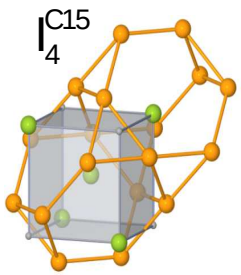


- 44 $\mu_B$

**Large AF moment**

## C15 Clusters

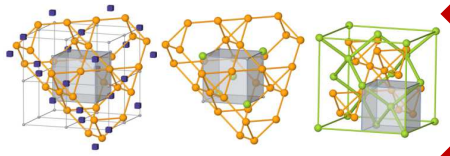

1. Very stable
2. Immobile
3. Can grow
4. Large AF moment

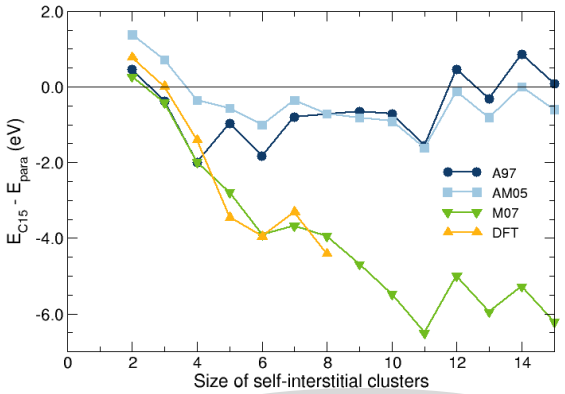


**Very stable**

$$I_n^{C15} + I_1^{\langle 110 \rangle} = I_{n+1}^{C15}$$

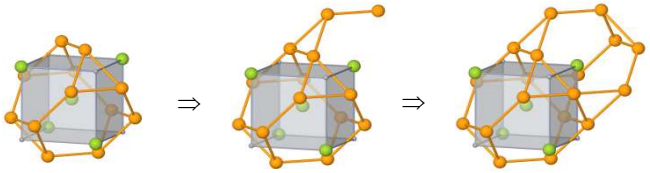

**Growth**

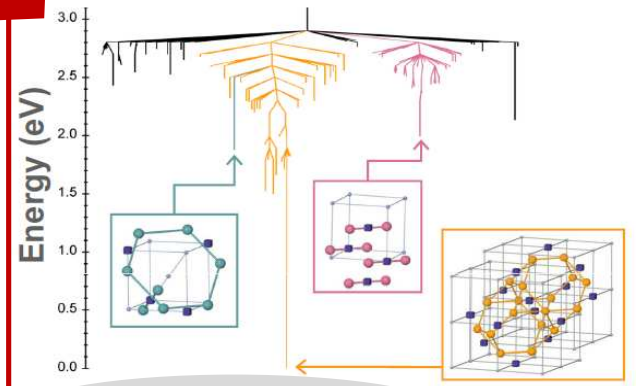


**Immobile**

# STABILITY OF C15 INTERSTITIAL CLUSTERS IN FE

Stability of C15 clusters against loops

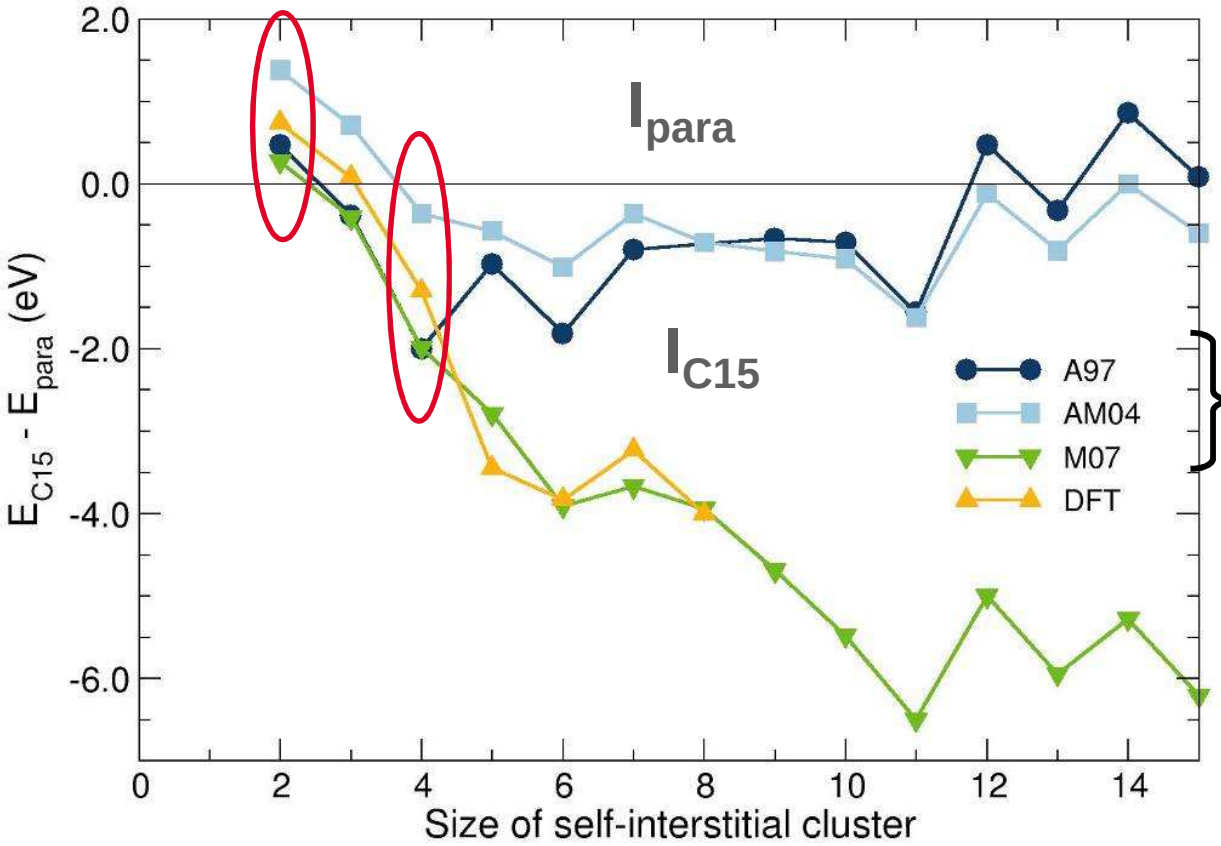


M07: improved by including in the fit a large data base of DFT defect properties (no C15 clusters)

EAM potentials

*Malerba et al. JNM 406, 19 (2010) with one typo corrected in: MCM et al, PRL 108, 025501 (2012)

DFT calculations: PWSCF code, 250 atoms, tested against pseudopotential (USPP and PAW), semicore states, LDA/GGA, cell size

# Others BCC: I4 case

1. Not in other bcc metals

2. Ta has interesting property

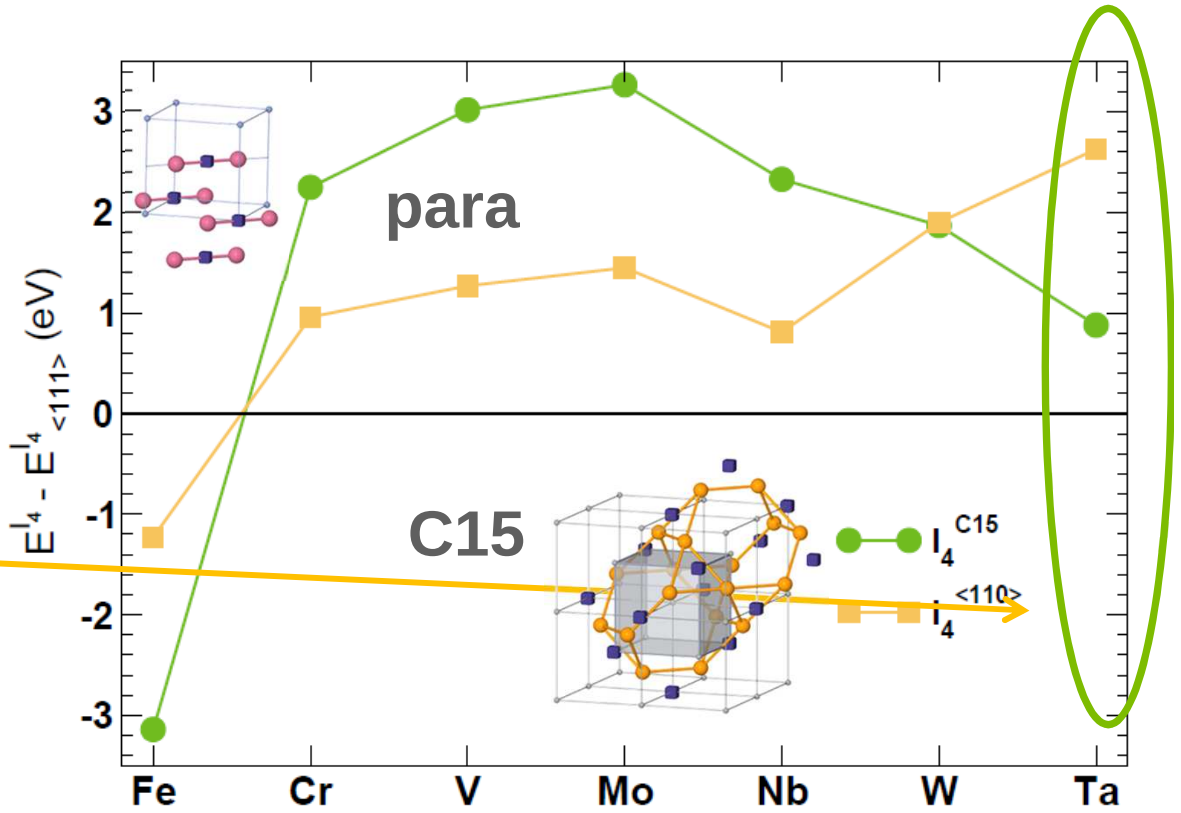

- M07 EAM potential for Fe
- Activation Relaxation Technique (ART)
- disconnectivity graph representation

O. M. Becker and M. Karplus, J. Chem. Phys. **106**, 1495 (1997)
D. J. Wales, M. A. Miller, and T. Walsh, Nature **394**, 758 (1998)

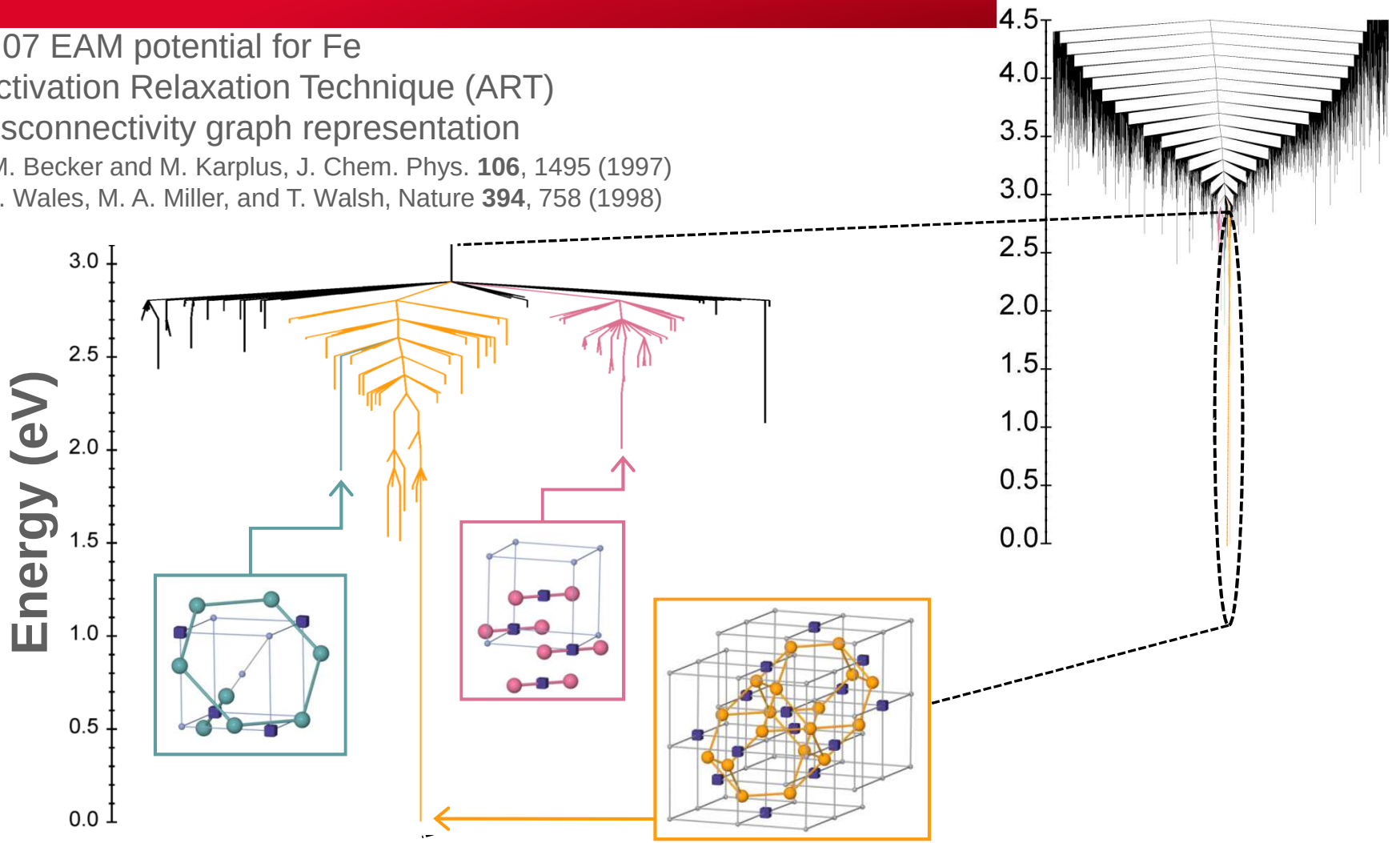


1. Two basins: C15 and parallel dumbells ; confirms that C15 is the lowest energy structure
2. shows that it is immobile (confirmed by MD simulation over μs)
3. . Older clusters identify a particular branch of the C15 basin

# Growth of C15 Clusters

$$I_n^{C15} + I_1^{\langle 110 \rangle} = I_{n+1}^{C15}$$

$I_2^{C15}$ 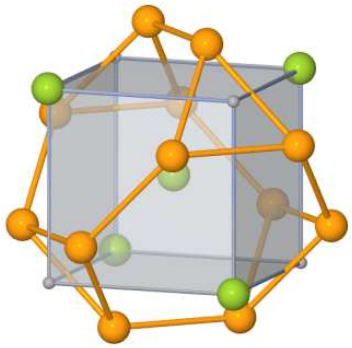 $\Rightarrow$ $I_3^{C15}$ 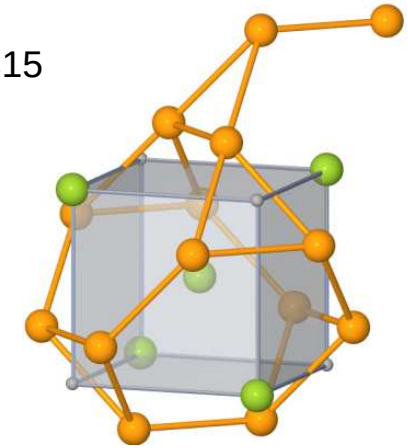 $\Rightarrow$ $I_4^{C15}$ 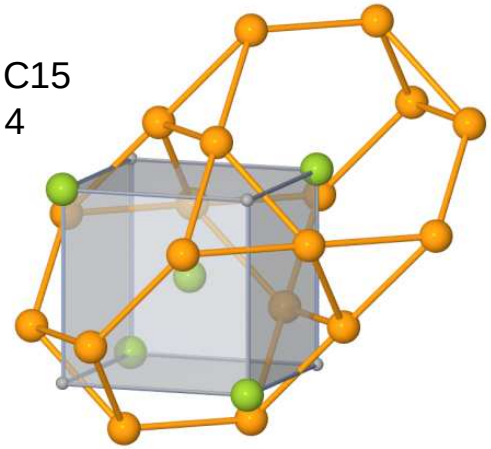

- ARTn

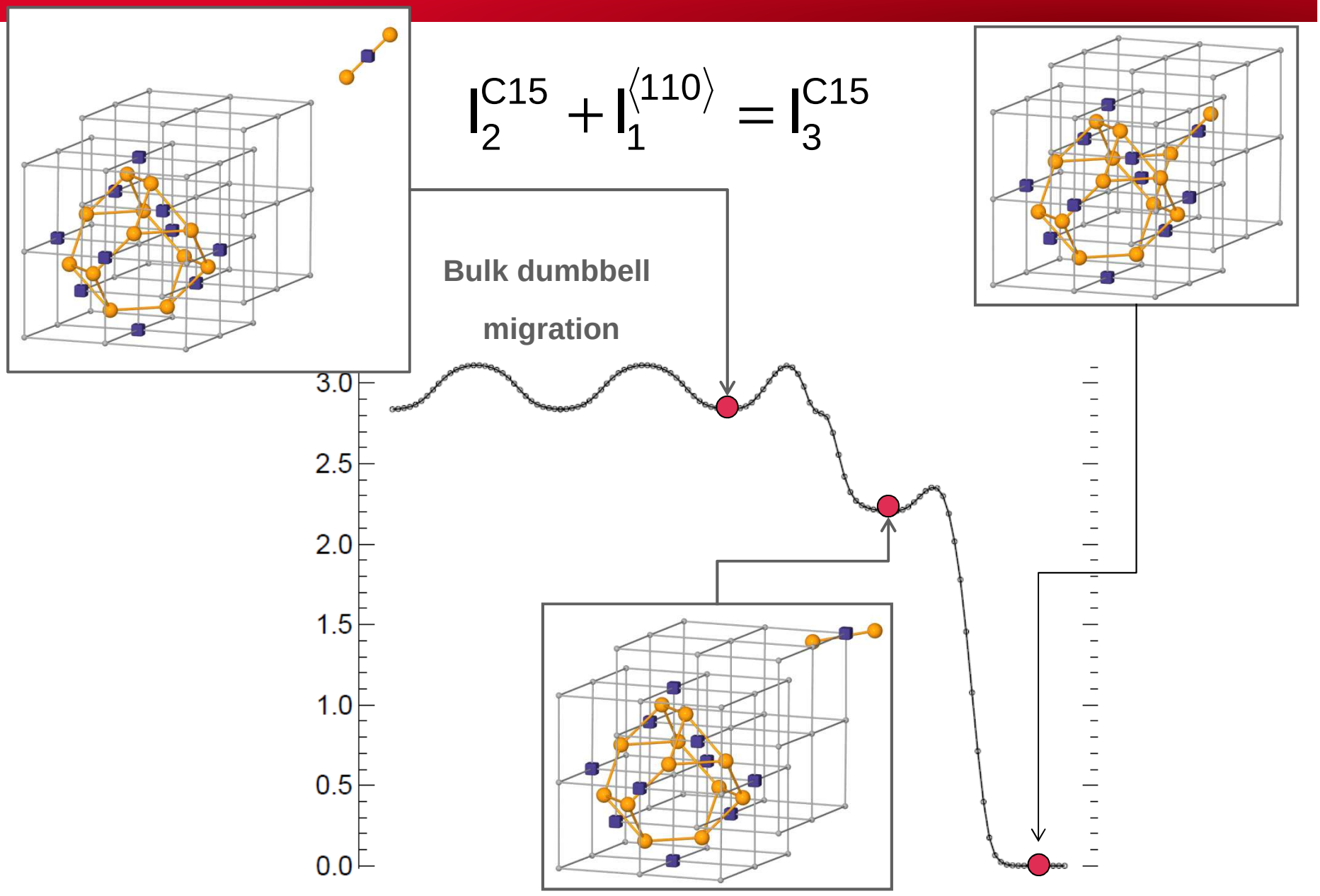


Doesn't exceed the barrier for <110> dumbbell migration

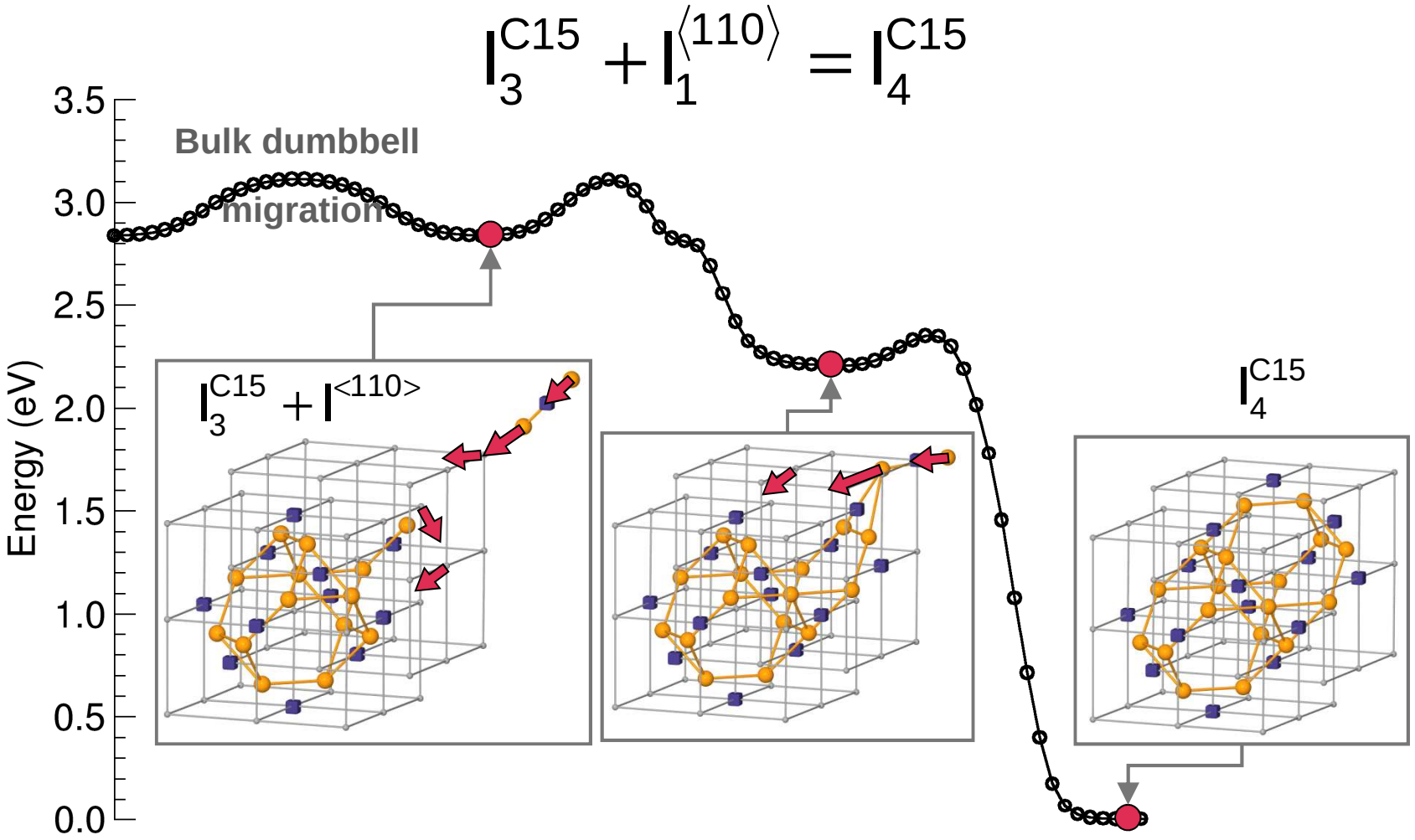


Doesn't exceed the barrier for <110> dumbbell migration

# SUMMARY

**Using a method for systematic search in the energy landscape we have predicted a 3D crystalline structure for self-interstitial clusters in bcc metals**

- Very low energy structures
- Can grow by capturing <110> dumbbells
- Have large antiferromagnetic moments in Fe
- Are immobile